European air quality maps of ozone and PM_{10}

for 2008

and their uncertainty analysis

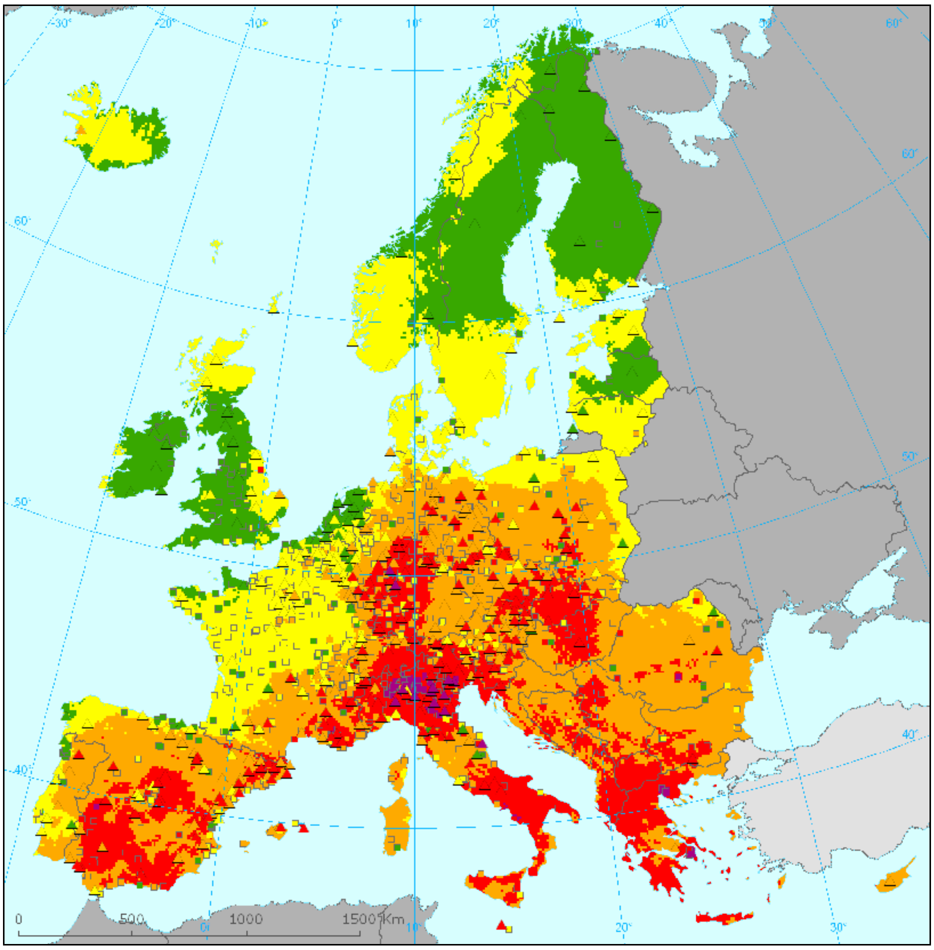

ETC/ACC Technical Paper 2010/10
December 2010

Peter de Smet, Jan Horálek, Markéta Coňková,
Pavel Kurfürst, Frank de Leeuw, Bruce Denby

European Topic Centre
on Air and Climate Change

The European Topic Centre on Air and Climate Change (ETC/ACC)
is a consortium of European institutes under contract of the European Environment Agency
PBL UBA-D UBA-V NILU AEAT AUTh CHMI MET.NO ÖKO TNO REC

Front page picture:
The ozone levels for the health indicators 26th highest daily maximum 8-hour value in µg.m^{-3} for both the rural and urban areas, combined into one final map for the year 2008. Its target value is 120 µg.m^{-3}. (Figure 5.1 of this paper).
Note the considerable decrease in areas with ozone levels above the target value compared to those of 2007 (ETC/ACC Technical Paper 2009/9 cover figure), 2006 (ETC/ACC Technical Paper 2008/8 cover figure), and 2005 (ETC/ACC Technical Paper 2007/7, cover figure).

Author affiliation:
Peter de Smet, Frank de Leeuw: Netherlands Environmental Assessment Agency (PBL until 31-12-2010), Bilthoven, The Netherlands
Jan Horálek, Markéta Coňková,Pavel Kurfürst: Czech Hydrometeorological Institute (CHMI), Praha, Czech Republic
Bruce Denby: Norwegian Institute of Air Research (NILU), Kjeller, Norway

Refer to this document as:
De Smet P, Horálek J, Coňková M, Kurfürst P, de Leeuw F, Denby B (2010). European air quality maps of ozone and PM10 for 2008 and their uncertainty analysis. ETC/ACC Technical paper 2010/10
http://air-climate.eionet.europa.eu/reports/ETCACC_TP_2010_10_spatAQmaps_2008

DISCLAIMER

ETC/ACC Technical Paper 2010/10
European Topic Centre on Air and Climate Change
PO Box 303
3720 AH Bilthoven
The Netherlands
Phone +31 30 2743550
Fax +31 30 2744433
Email etcacm@rivm.nl
Website http://acm.eionet.europa.eu/

Contents

1 Introduction

This paper provides an update of the European air quality concentrations of selected pollutants, their exceedance probability and population exposure estimates for another consecutive year, 2008. The analysis is based on interpolation of annual statistics of the 2008 observational data reported by EEA Member countries in 2009. The paper presents the mapping results and includes an uncertainty analysis of the interpolated maps, building upon the latest methodological developments of Horálek et al. (2007, 2008, 2010) and De Smet et al. (2009, 2010).

We consider in this paper again PM_{10} and ozone, as being the most relevant pollutants for annual updating. However, $PM_{2.5}$ is also an important policy relevant pollutant and health impact indicator, its mapping is considered a theme still under development and is dealt with in separate ETC/ACC Technical Papers (De Leeuw and Horálek, 2009; Denby and Gola, 2010) and a scientific article (De Leeuw et al. (2010).

Apart from minor methodological improvements and updated data sources, the analysis of the year 2008 is similar to that of the year 2007. In this paper, we discuss just the methodological changes and data updates applied to 2008 data. ETC/ACC Technical Paper 2009/9 (De Smet et al. 2010) provides more details on the background of the analysis, its applied methodologies and data sources. The methodological changes we introduce in this paper involve the recommendations of ETC/ACC Technical Paper 2009/16 (Horálek et al., 2010).

Next to annual indicator maps, we present in tables the population exposure to PM_{10} and ozone and the exposure of vegetation to ozone. These tables are prepared on the basis of 1x1 km^2 grid resolution of both the combined final maps and the population density map.

For all the maps, we include a quantitative estimate of their interpolation uncertainty, using cross-validation parameters and scatter-plots. In addition, the paper contains the maps with probability estimates of limit/target value exceedances. For presentational purposes on European scale we aggregated the 1x1 km^2 grids into maps of a 10x10 km^2 grid resolution, leading to considerably smaller figure file sizes.

Chapter 2 describes briefly the applied changes in methodology. Chapter 3 documents the updated input data. Chapters 4 and 5 present the calculations, the mapping, the exposure estimates and the uncertainty results for PM_{10} and ozone respectively. Chapter 6 summarizes the conclusions on exposure estimates and their interpolation uncertainties involved with the interpolated mapping of the air pollutant indicators.

2 Methodological changes

Methodological process

Previous technical papers prepared by the ETC/ACC (Technical Papers 2009/16, 2009/9 2008/8, 2007/7, 2006/6, 2005/8 and 2005/7) discuss methodological developments and details on spatial interpolations and their uncertainties. The latest papers represent the latest status of the methodological details we apply now. In this paper, we introduce the recommendations of ETC/ACC Technical Paper 2009/16 (Horálek et al., 2010) for the first time. It involves some minor methodological changes we summarise here.

The mapping method applied, includes creating separately a rural map from rural background observational data, an urban map from urban and suburban background station data, and a joint rural/urban map from the data of all background stations regardless their type. These maps we create on a European scale of 10x10 km^2 grid resolution, except for the AOT40 maps used for the EEA Core Set Indicator 005 based on a 2x2 km^2 grid resolution. Each map type has been derived with the same *spatial interpolation* method as used before with the only modification a lognormal transposition of PM_{10} annual average and 36th maximum daily average data prior to the interpolation. Interpolation on lognormal PM_{10} data provides some improved interpolation results compared to the previously used normal PM_{10} data. For ozone the lognormal transposition brings no improvement and is not implemented. The spatial interpolation consists of a linear regression with ordinary kriging of its residuals based on a variogram estimate using a spherical function (with parameters: nugget, sill, range).

Subsequently, we derive grid by grid a final combined map from the separate maps by applying selection criteria and a weighting function. This *'merging'*-process happens from this year onward, according the recommendations of Horálek et al. (2010), on the basis of:

- a population density map on a higher 1x1 km^2 grid resolution, instead of the previously used 10x10 km^2;
- a somewhat better fine-tuned weighting criteria of Equation 5.1, instead Equation 2.3 in Horálek et al. (2010).

For the *health exposure assessment* per country and for Europe as a whole we now derive the population averaged concentrations and exceedance exposures by using the combined final concentration map and the population density on the higher 1x1 km^2 grid resolution, instead of the previously used 10x10 km^2 grid resolution. The *vegetation exposures* are still calculated on the basis of the air quality maps and CLC2000 land cover data, both at a 2x2 km grid resolution.

Log-normal concentration transposition

In the case of PM10 we logarithmically transform concentrations from both the air quality measurements and the EMEP modelling output. Then we apply the multiple linear regression, followed by residual kriging, using (Equation 2.4 of Horálek et al. (2010)):

$$\hat{Y}(s_0) = c + a_1 \ln(X_1(s_0)) + a_2 X_2(s_0) + ... + a_n X_n(s_0) + \eta(s_0) \qquad (2.1)$$

where $\hat{Y}(s_0)$ is the estimated value of the logarithmical transformed concentration at point s_o

$X_1(s_0)$ is the output of dispersion model at point s_o

$X_2(s_0),\ldots, X_n(s_0)$ are the other supplementary variables at point s_o

$c, a_1, a_2,,\ldots, a_n$ are the $n+1$ selected parameters of the linear regression model calculated at the point of measurement s_0,

$\eta(s_0)$ is the spatial interpolation of the residuals of the linear regression model at the point of measurement.

The interpolated values are back-transformed by exponentiation with the kriging error:

$$\hat{Z}(s_0) = \exp\left\{Y(s_0) + \frac{\sigma^2(s_0)}{2}\right\} \tag{2.2}$$

where $\hat{Z}(s_0)$ is the estimated back-transformed concentration value at point s_0

$\sigma(s_0)$ is the kriging error value at point s_0.

The back-transformed standard error of the interpolation is calculated (Denby et al., 2008):

$$\delta(s_0) = \sqrt{\exp\left(\sigma^2(s_0) - 1\right)\exp\left\{2Y(s_0) + \sigma^2(s_0)\right\}} \tag{2.3}$$

where $\delta(s_0)$ is the back-transformed standard error of the interpolation at point s_0.

This back-transformed standard error is subsequently used in the probability of exceedance map, as presented in Horálek et al. (2008), Equation 2.1.

Refined selection and weighting criteria at merging

The increased grid resolution for merging contributes significantly to the accuracy of specific areas with small urbanisations in predominantly rural areas.

In the case of the PM_{10} indicators, the combined final European map has been composed so far from the separate maps according the grid value selection and weighting criteria reflected in Equation 2.3 of Horálek et al. (2010):

$$
\begin{aligned}
\hat{Z}(s_0) &= \hat{Z}_r(s_0) && \text{for } \alpha(s_0) \le \alpha_1 \text{ and } \hat{Z}_r(s_0) \le \hat{Z}_u(s_0) \\
&= \hat{Z}_u(s_0) && \text{for } \alpha(s_0) \ge \alpha_2 \text{ and } \hat{Z}_r(s_0) \le \hat{Z}_u(s_0) \\
&= \frac{\alpha_2 - \alpha(s_0)}{\alpha_2 - \alpha_1} \cdot \hat{Z}_r(s_0) + \frac{\alpha(s_0) - \alpha_1}{\alpha_2 - \alpha_1} \cdot \hat{Z}_u(s_0) && \text{for } \alpha_1 < \alpha(s_0) < \alpha_2 \text{ and } \hat{Z}_r(s_0) \le \hat{Z}_u(s_0) \\
&= \hat{Z}_j(s_0) && \text{for } \hat{Z}_r(s_0) > \hat{Z}_u(s_0)
\end{aligned} \tag{2.4}
$$

where $\hat{Z}(s_0)$ is the estimated value of concentration at point s_o

$\hat{Z}_r(s_0)$ is the concentration at point s_o for the rural map, based on the rural background stations only

$\hat{Z}_u(s_0)$ is the concentration at point s_o for the urban map, based on the urban and suburban background stations only

$\hat{Z}_j(s_0)$ is the concentration at point s_o for the joint urban/rural map, based on all background stations

$\alpha(s_o)$ is the density of population at point s_o

α_1, α_2 are the population density classification interval parameters, set as $\alpha_1 = 100$ inhbs.km^{-2} and $\alpha_2 = 500$ inhbs.km^{-2}.

The final map for ozone indicators was calculated similarly, but with *opposite* conditions for the relation between $\hat{Z}_r(s_0)$ and $\hat{Z}_u(s_0)$.

Whereas in general one can assume that the joint urban/rural grid value should be in between the corresponding urban and rural grid value, it appears in some situations not to be the case. Reasons for such deviation are that different supplementary variables or different kriging parameters have been used to create the individual urban, rural and joint urban/rural map. To eliminate this discrepancy, we prescribe now that grid cell values of this joint rural/urban map should fall within the interval of the corresponding grid cell values of the separate rural and urban map. For PM_{10} this means that Equation 5.1 of Horálek et al (2010) has to be more precisely specified as:

$$\begin{aligned}
\hat{Z}(s_0) &= \hat{Z}_r(s_0) && \text{for } (\hat{Z}_r(s_0) \leq \hat{Z}_u(s_0) \text{ and } \alpha(s_0) \leq \alpha_1) \text{ or } \hat{Z}_j(s_0) > \hat{Z}_r(s_0) > \hat{Z}_u(s_0) \\
&= \hat{Z}_u(s_0) && \text{for } (\hat{Z}_r(s_0) \leq \hat{Z}_u(s_0) \text{ and } \alpha(s_0) \geq \alpha_2) \text{ or } \hat{Z}_r(s_0) > \hat{Z}_u(s_0) > \hat{Z}_j(s_0) \\
&= \frac{\alpha_2 - \alpha(s_0)}{\alpha_2 - \alpha_1} \cdot \hat{Z}_r(s_0) + \frac{\alpha(s_0) - \alpha_1}{\alpha_2 - \alpha_1} \cdot \hat{Z}_u(s_0) && \text{for } \hat{Z}_r(s_0) \leq \hat{Z}_u(s_0) \text{ and } \alpha_1 < \alpha(s_0) < \alpha_2 \\
&= \hat{Z}_j(s_0) && \text{for } \hat{Z}_r(s_0) > \hat{Z}_u(s_0) \text{ and } \hat{Z}_r(s_0) \geq \hat{Z}_j(s_0) \geq \hat{Z}_u(s_0)
\end{aligned} \quad (2.5)$$

For ozone the similar equation applies with *opposite* conditions for the relation between $\hat{Z}_r(s_0)$, $\hat{Z}_u(s_0)$ and $\hat{Z}_j(s_0)$.

Optimised application of spatial resolution in the process steps

In summary, the different spatial grid resolutions we apply now in the three process steps (*interpolation – merging – exposure estimates*) to obtain the ultimate health exposure assessment are based on the most optimal combination of grid resolutions (*10-1-1*), instead of the previously used (*10-10-10*), meaning we implement the recommendations of Horálek et al. (2010):

- *Interpolation*: Calculate the three separate urban, rural and joint concentration maps on a 10x10 km^2 grid resolution. One loses little to no significant information against considerably reduced computational demand, compared to maps calculated on a 1x1 km^2 grid resolution. (Nevertheless, bearing in mind that the AOT40 maps are already routinely calculated at the 2x2 km^2 grid resolution for more accurate ozone impact estimates of the EEA CSI indicators, one could for consistency reasons consider to introduce this refinement in the near future.)
- *Merging*: Subsequently, merge these separate maps on basis of the 1x1 km^2 population density map into a 1x1 km^2 combined final concentration map, instead of merging on 10x10 km^2 grid resolution. Refining the grid resolution improves the accuracy of the obtained combined final concentration map both for PM_{10} and ozone, rather indifferent from resolution of the separate interpolated maps. It better accounts for smaller urbanisations in predominantly rural areas. The resolution at merging plays a substantial role in these improvements, as opposed to the resolution of the separate interpolated maps. (This led to the implementation at both PM_{10} and ozone of a finer resolution at merging only, not at interpolation. There we maintain the computational less demanding interpolations of the separate maps on the 10x10 km^2 grid resolution).
- *Exposure estimates*: Finally, we derive population averaged concentrations and exceedance exposures using the population density map with the 1x1 km^2 grid resolution. (Spatial aggregation causes a considerable decreased accuracy in the accounting for population averaged concentrations and exceedance exposures. This methodological adverse 'thinning'-effect should be avoided at all times.)

The combination (*10-1-1*) is used primarily for exposure estimates. For presentational purposes of European map pictures a spatially aggregation to 10x10 km^2 grids is preferred (see below). The aggregation reduces the map figure and file sizes considerably. In addition, in case 1x1 km^2 maps would be needed for presentational purposes, at combination (*10-1-1*) the possibility exists that 10x10 km^2 square-like patterns would 'show through' in the map. These originate from the separate rural and urban maps that resulted from the interpolation on the 10x10 km^2 resolution. To avoid this, one should use then combination (*1-1-1*).

Furthermore, the estimation of the interpolation uncertainties and probability of exceedances (PoE) takes place on the spatially aggregated 10 x10 km^2 gridded concentration map, since that represents the original resolution of the interpolation. The aggregation involves the following equation 2.6:

$$\begin{aligned}\hat{Z}(s_0) &= \frac{1}{100}\sum_{i=1}^{100}\left(\frac{\alpha_2-\alpha(s_{0i})}{\alpha_2-\alpha_1}\cdot\hat{Z}_r(s_0)+\frac{\alpha(s_{0i})-\alpha_1}{\alpha_2-\alpha_1}\cdot\hat{Z}_u(s_0)\right)\\ &= \hat{Z}_r(s_0).\left(\frac{1}{100}\sum_{i=1}^{100}\frac{\alpha_2-\alpha(s_{0i})}{\alpha_2-\alpha_1}\right)+\hat{Z}_u(s_0).\left(\frac{1}{100}\sum_{i=1}^{100}\frac{\alpha(s_{0i})-\alpha_1}{\alpha_2-\alpha_1}\right)\\ &= \hat{Z}_r(s_0).w'_r(s_0)+\hat{Z}_u(s_0).w'_u(s_0)\end{aligned} \tag{2.6}$$

where $\hat{Z}(s_0)$ is the estimated value of concentration at 10x10 km^2 grid cell s_o

$\hat{Z}_r(s_0)$ is the concentration at 10x10 km^2 grid cell s_o for the rural map

$\hat{Z}_u(s_0)$ is the concentration at 10x10 km^2 grid cell s_o for the urban map

$\alpha(s_{oi})$ is the density of population at 1x1 km^2 grid cell s_{oi}

α_1, α_2 are the population density classification interval parameters, set as $\alpha_1 = 100$ inhbs.km^{-2} and $\alpha_2 = 500$ inhbs.km^{-2}

$w'_r(s_0), w'_u(s_0)$ are the rural and urban weights at 10x10 km^2 grid cell s_o.

The probability of exceedances (PoE) is estimated on the same aggregated resolution using equation 2.2 in Horálek et al. (2008), i.e.

$$\delta_c = \sqrt{w_r'^2\cdot\delta_r^2 + w_u'^2\cdot\delta_u^2 + 2w'_r\cdot w'_u\cdot\delta_r\cdot\delta_u\cdot r_{ru}} \tag{2.7}$$

where δ_c is the combined uncertainty (standard deviation) in the 10x10 km^2 grid cell

$w'_r(s_0)$ is the weight factor based on population density for the rural grid cells

$w'_u(s_0)$ is the weight factor based on population density for the rural grid cells

δ_r and δ_u are the uncertainties in the corresponding rural resp. urban grid cell

r_{ru} is the correlation coefficient of the rural and urban concentration fields.

There is an additional option for improving interpolations and impact assessment not dealt with in this paper, but certainly relevant for consideration in relation to the chosen merging resolution. Therefore, we address it here briefly. An alternative lower value for the rural class boundary of $\alpha_1 = 50$ inhbs.km^{-2}, instead of the current 100 inhbs.km^{-2}, provides improved interpolated maps and subsequently improved impact assessments. Specifically one obtains improved interpolations for the mapping of small towns and cities in predominantly and more sparsely populated rural areas. It reduces the uncertainties caused by 'overlooking' small urbanisations in the more extended rural areas, which we had detected as most likely one of the weakest points in the current mapping methodology. Therefore, the use of $\alpha_1 = 50$ inhbs.km^{-2} could be recommended to be introduced as part of the default merging methodology at both PM10 and ozone, if the 10x10 km^2 merger would still be applied in the mapping methodology. However, the use of a merger with finer 1x1 km^2 grid resolution will be considerably more effective to resolve the overlooking of small cities in lower and moderately populated areas than the use of an alternative population density class boundary for the rural areas. Nevertheless, this alternative class boundary could be used at occasions where the application of the 1x1 km^2 grid resolution merger would become too computational and time demanding. For example, it could be used when 'quick and dirty' draft map impressions or presentations are preferred over the more accurate maps.

3 Input data

The set of sources of input data in this paper differs not from De Smet et al. (2010). The air quality, meteorological and, where possible, the supplementary data has been updated. No further changes in selecting and processing the input data have been made. For readability of this paper we reproduce here the list of the input data. The key data is the air quality measurements at the monitoring stations extracted from AirBase. The supplementary data covers the whole mapping domain and is converted into the reference EEA ETRS89-LAEA5210 projection on a 10x10 km^2 grid resolution. Except for the AOT40 maps for which the data was – as last year – converted into a 2x2 km^2 grid resolution to allow accurate land cover exposure estimates to be used in when calculating the CSI005 indicator of EEA.

3.1 Measured air quality data

Air quality 2008 station monitoring data is extracted from the European monitoring database AirBase (Mol et al. 2010),supplemented by several rural EMEP stations not reported to AirBase. Only data from stations classified by AirBase and/or EMEP of the type *background* for the areas *rural*, *suburban* and *urban* are used. *Industrial* and *traffic* station types are not considered; they represent local scale concentration levels not applicable at the mapping resolution employed. The following components and their indicators are considered:

PM_{10} – annual average [$\mu g.m^{-3}$], year 2008
– 36^{th} maximum daily average value [$\mu g.m^{-3}$], year 2008

Ozone – 26^{th} highest daily maximum 8-hour average value [$\mu g.m^{-3}$], year 2008
– SOMO35 [$\mu g.m^{-3}$.day], year 2008
– AOT40 for crops [$\mu g.m^{-3}$.hour], year 2008
– AOT40 for forests [$\mu g.m^{-3}$.hour], year 2008

SOMO35 is the annual sum of maximum daily 8-hour concentrations above 70 $\mu g.m^{-3}$ (i.e. 35 ppb). AOT40 is the sum of the differences between hourly concentrations greater than 80 $\mu g.m^{-3}$ (i.e. 40 ppb) and 80 $\mu g.m^{-3}$, using only observations between 7:00 and 19:00 UTC, calculated over the three months from May to July (AOT40 for crops), respectively over the six months from April to September (AOT40 for forests). Note that the term *vegetation* as used in the ozone directive is not further defined. Comparing the definitions in the Mapping Manual (UNECE, 2004) and those in the ozone directive suggests that we have to interpret the term *vegetation* in the ozone directive as agricultural crops. The exposure of *agricultural crops* has been evaluated here on basis of the AOT40 for vegetation as defined in the ozone directive.

For the indicators relevant to human health (i.e. PM_{10}, and for ozone the 26^{th} highest daily maximum 8-hour average and SOMO35) data from *rural*, *urban* and *suburban* background stations is considered. For the indicators relevant to vegetation damage (both AOT40 indicators for ozone) only *rural* background stations are considered.

Only the stations with annual data coverage of at least 75 percent are used. We excluded the stations from French overseas areas (departments), Svalbard, Azores, Madeira and Canary Islands. These areas were excluded from the interpolation and mapping domain. To reach a more extended spatial coverage by measurement data we used, in addition to the AirBase data, seven additional rural background PM_{10} stations from the EMEP database. Table 3.1 shows the number of the measurement stations selected for the individual pollutants and their respective indicators. Compared to 2007, the number of stations selected for 2008 increased for the PM_{10} health indicators by approximately 12 % for rural and 21 % for urban background stations; for the ozone health indicators the increase was about 15 % and for both AOT40 indicators approximately 18 %.

Table 3.1 Number of stations selected for the individual indicators and areas. For rural areas the rural background stations and for urban areas the urban and suburban background stations are used.

	PM10		ozone			
	annual average	36th daily maximum	26th highest daily max. 8h	SOMO35	AOT40 for crops	AOT40 for forests
rural	269	269	480	480	488	491
urban	1058	1058	988	988		

3.2 Unified EMEP model output

The chemical dispersion model used here is the Unified EMEP model (revision rv3_7_hirlam), which is a Eulerian model with a resolution of 50 x 50 km. This model provides information on a 50 km x 50 km scale, which was disaggregated to the 10x10km^2 grid cells according section 4.4 in Horálek et al. (2007). The model output parameters consist of the same set as the air quality measurement parameters (2008 data extracted in October 2010):

PM_{10} – annual average [µg.m^{-3}], year 2008
– 36th maximum daily average value [µg.m^{-3}], year 2008

Ozone – 26th highest daily maximum 8-hour average value [µg.m^{-3}], year 2008
– SOMO35 [µg.m^{-3}.day], year 2008
– AOT40 for crops [µg.m^{-3}.hour], year 2008
– AOT40 for forests [µg.m^{-3}.hour], year 2008

Simpson et al. (2003), Fagerli et al. (2004) and http://www.emep.int/OpenSource/index.html (EMEP web site) describe the model in more detail. The model results are based on emissions for the relevant year (Mareckova et al. 2010) and actual meteorological data (from HIRLAM numerical weather prediction model, version 7.1.3). Benedictow et al. (2010) provides further details on the EMEP modelling for 2008.

3.3 Altitude

We use the altitude data field (in meters) of GTOPO30 that covers the European continent, with an original grid resolution of 30 x 30 arcsec. This data was converted into 200 x 200 m^2 grid resolution. For details, see Horálek et al. (2007). This output was spatially aggregated into the reference 10 km x 10 km grid.

3.4 Meteorological parameters

Actual meteorological surface layer parameters are extracted from the Meteorological Archival and Retrieval System (MARS) of the ECMWF (European Centre for Medium-range Weather Forecasts). The derived parameters currently used and extracted from the ECMWF variables (details specified in Horálek et al. 2007, Section 4.5) are:

Wind speed – annual average [m.s^{-1}], year 2008
Surface solar radiation – annual average [MWs.m^{-2}], year 2008

3.5 Population density

Population density [inhbs.km^{-2}], census 2001, is based on JRC data for the majority of countries (JRC, 2009) – source EEA, pop01clcv5.tif, official version 5, 24 Sep. 2009, resolution 100x100 m^2.

For countries (Andorra, Albania, Bosnia-Herzegovina, Iceland, Liechtenstein, FYR of Macedonia, Montenegro, Norway, Serbia, Switzerland and Turkey) and regions (Faroe Islands, Jersey, Guernsey, Man, Gibraltar, and northern part of Cyprus) which are not included in this map we used population density data from an alternative source, namely the ORNL LandScan (2002) Global Population Dataset.

The ORNL data is reprojected and converted from its WGS1984 30x30 arcsec grids into EEA's reference projection ETRS89-LAEA5210 on a 1x1 km^2 grid resolution. Furthermore, the data is compared on the one hand with JRC data for countries covered by both data sources, and on the other hand with Eurostat national population for 2008 (Eurostat, 2008). Based on these comparisons, showing good agreement of JRC and Eurostat data, but underestimation of ORNL reprojected data, a multiplication factor 1.49 has been applied for all ORNL reprojected data, which assures a better match with the levels of JRC data. The conversion introduced most likely the underestimation. Figure 3.1 presents this comparison between JRC and ORNL data based on the national population totals of the individual countries.

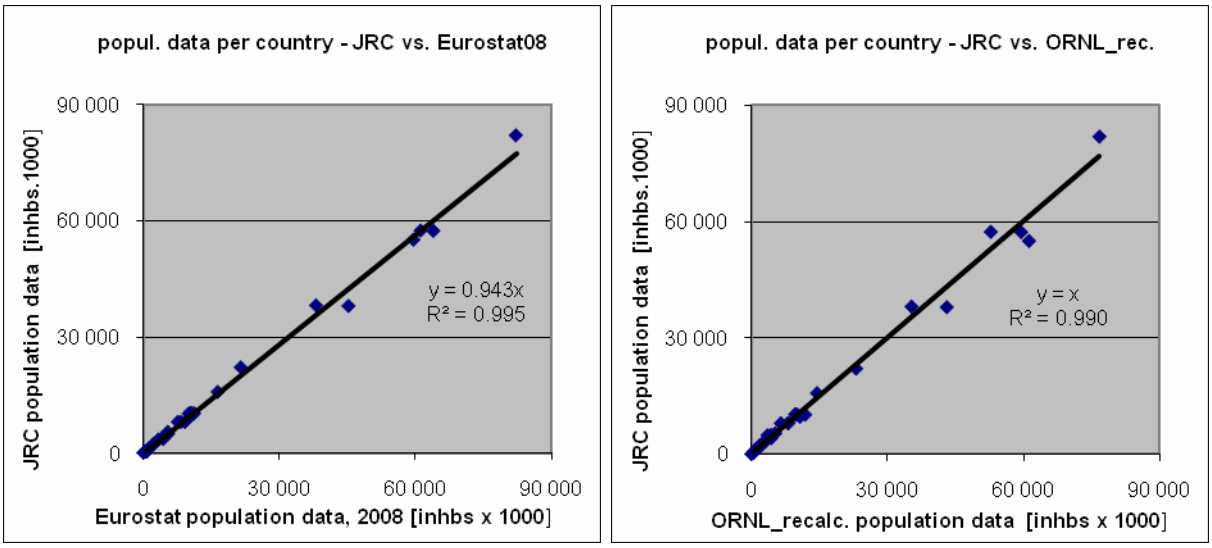

Figure 3.1 Correlation between JRC (y-axis) and the Eurostat 2008 revision (x-axis, left), respectively ORNL recalculated (x-axis, right) national population totals.

The population density data was used to classify the spatial distribution of the type of areas (rural, urban or mixed population density) in Europe. We use it to select and weight grid by grid, from the separate rural, urban and joint rural/urban maps, the air quality value to that has be assigned to the grid squares of the final combined air quality map. Furthermore, we use it to estimate the ultimate population health exposure and exceedance numbers per country and Europe as a whole, including involved uncertainties. These activities take place on a 1x1 km^2 grid resolution as implementation of the recommendations of Horálek et al. (2010). For presentational purposed we construct the maps on a 10x10 km^2 grid resolution. To facilitate all this, we spatially aggregated the JRC 100x100 m^2 population density data into a 1x1 km^2 grid, merged that with the ORNL dataset, and aggregated that into an additional 10x10 km^2 grid map.

3.6 Land cover

The input data from CORINE Land Cover 2000 – grid 100 x 100 m^2, version 13 (2/2010) is used (CLC2000 V13 – 100m, g100_00.zip; EEA, 2010). The countries missing in this database are Andorra, Switzerland and Turkey. For Switzerland we use the preliminary data provided by ETC-LUSI (ETC-LUSI, 2010).

4 PM_{10} maps

This chapter presents the updates of 2008 for the interpolated map and exposures of the two PM_{10} health indicators annual average and 36th highest maximum daily average. The concentration maps and population exposure tables are calculated in the standard EEA ETRS89-LAEA5210 1x1 km^2 grid resolution. All the maps are presented in the standard EEA ETRS89-LAEA5210 10x10 km^2 grid resolution.

4.1 Annual average

4.1.1 Concentration map

Figure 4.1 presents the combined final map for the 2008 PM_{10} annual averages as the result of the interpolation and merging of the separate maps as described in detail in De Smet (2010) and Horálek et al. (2007). The red and purple areas and stations exceed the limit value (LV) of 40 $\mu g.m^{-3}$. Supplementary data in the regression used for rural areas is EMEP model output, altitude, wind speed and surface solar radiation, and for urban areas it is EMEP model output only. (The relevant linear regression submodels have been identified earlier in Horálek et al. (2008) and De Smet et al. (2009, 2010) as P.Eawr and UP.E, respectively).

The estimated parameters of the linear regression models (c, a_1, a_2,…) and of the residual kriging (*nugget, sill, range*) are presented in Table 4.1, including the statistical indicators of both the regression and the kriging. The adjusted R^2 and standard error are indicators for the fit of the regression relation, where the adjusted R^2 should be as close to 1 as possible and the standard error should be as small as possible. The adjusted R^2 is 0.29 for the rural areas and 0.00 for urban areas. However, in reality no linear regression has been applied for the urban areas due to non-significance of the only supplementary data source. The R^2 values show a slightly poorer fit of the regression than observed for year 2007 (0.40 and 0.10), but better fit on rural for the years 2006 (0.29 and 0.03) and 2005 (0.28 and 0.06) (De Smet et al. 2010 and 2009, Table 4.1; Horálek et al. 2008, Tables A.21 and A2.6). These low values for urban areas over the years indicate that the fit of the regression in urban areas is poor (Horálek et al. 2007, 2008; De Smet et al. 2009, 2010). RMSE and MPE are the cross-validation indicators, showing the quality of the resulting map; the MPE indicates to what extent the estimation is un-biased. Section 4.1.3 deals with more detailed analysis and compares with results of 2007, 2006 and 2005.

Table 4.1 Parameters of the linear regression models (Eq. 2.1) and of the ordinary kriging variograms (nugget, sill, range) - and their statistics - of PM_{10} indicator annual average for 2007 in the rural (left) and urban (right) areas as used for the combined final map, i.e. rural linear regression model P.Eawr (left), resp. urban UP.E (right) followed by interpolation of its regression residuals using ordinary kriging (OK; coded with 'a').

linear regr. model + OK on its residuals	rural areas (lnP.Eawr-a)	urban areas (lnUP.E-a)
	coeff.	coeff.
c (constant)	2.38	3.25
a1 (log. EMEP model 2008)	0.301	n. sign.
a2 (altitude GTOPO)	-0.00047	
a3 (wind speed 2007)	-0.127	
a4 (s. solar radiation 2008)	0.042	
adjusted R^2	**0.29**	**0.00**
standard error [µg.m^{-3}]	**0.33**	**0.38**
nugget	0.04	0.02
sill	0.11	0.07
range [km]	600	330
RMSE [µg.m^{-3}]	**5.03**	**6.32**
MPE [µg.m^{-3}]	**0.15**	**0.00**

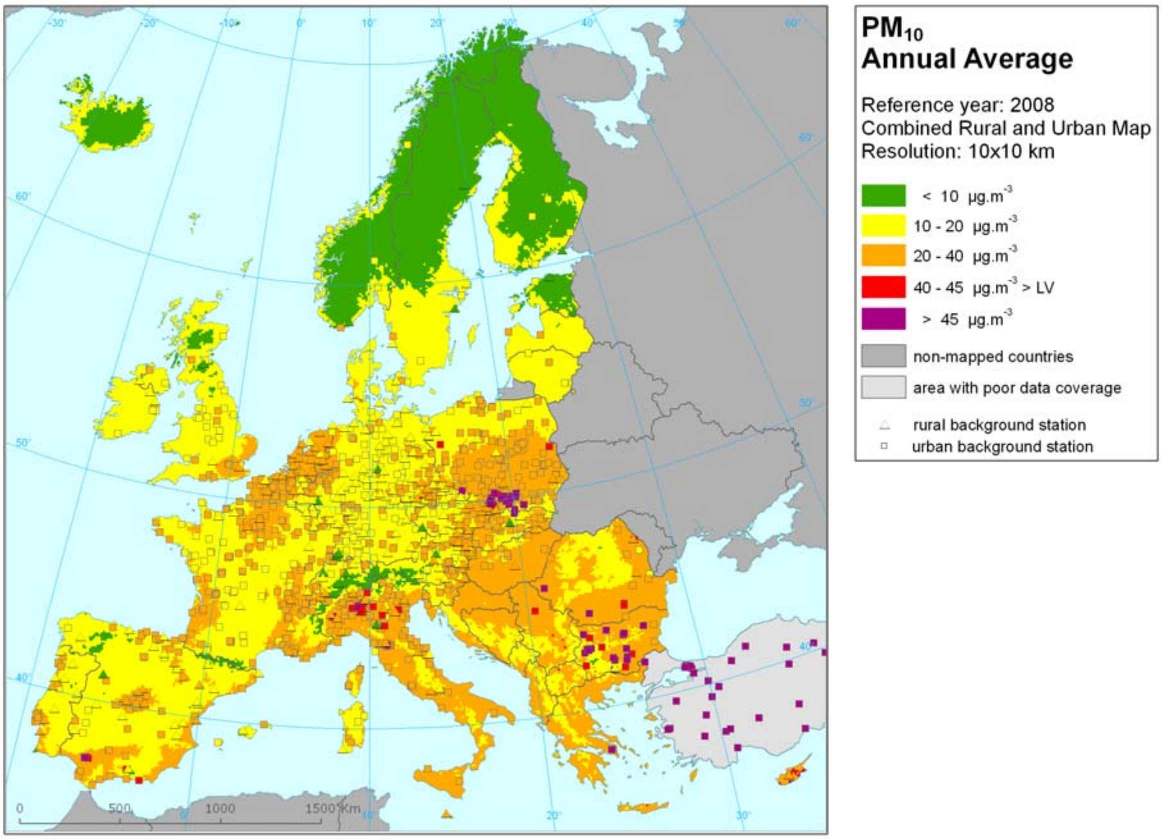

Figure 4.1 Combined rural and urban concentration map of PM_{10} – annual average, year 2008. Spatial interpolated concentration field and the measured values in the measuring points. Units: $\mu g.m^{-3}$.

4.1.2 Population exposure

Table 4.2 gives the population frequency distribution for a limited number of exposure classes calculated on a 1x1 km^2 grid resolution, as well as the population-weighted concentration (i.e. the average concentration per inhabitant) for individual countries and for Europe as a whole according to Equation 2.2 of De Smet et al. (2010).

Whereas previously the merging of the separate rural and urban map took place on a 10x10 km^2 grid resolution based on a 10x10km^2 population density map, from this year onward this merging takes place on a 1x1 km^2 grid of the population density map. It should be explicitly emphasized that the application of this increased resolution induces a shift in the distribution of population over the different exposure classes as well as in the population-weighted concentrations. This will perturb the comparison of current 2008 distributions with those of previous years. Nevertheless, comparison between years has been carried out since tendencies within and between countries and regions seem not to deviate significantly between 2008 and previous years.

About 30 % of the European population has been exposed to annual average concentrations below 20 $\mu g.m^{-3}$, the WHO air quality guideline. Almost two-thirds (63 %) of the European population lived in 2008 in areas where the PM_{10} concentration is estimated to be between 20 and 40 $\mu g.m^{-3}$. About 6 % of the population lived in areas where the PM_{10} annual limit value is exceeded, with Bulgaria, Cyprus, FYR of Macedonia and Serbia showing in 2008 a population weighted concentration and a median above the LV. However, as the next section discusses, the current mapping methodology tends to underestimate high values. Therefore, the exceedance percentage will most likely be higher and cause exceedance at a few more countries, for example Greece.

The frequency distribution shows a large variability over Europe, with a considerable increase for specifically those countries that showed also in 2007 exposures above limit values. Bulgaria, FYR of Macedonia and Serbia with more than one fifth above LV in 2007, do show in 2008 estimates of about two-third or more population exposure above LV. Romania is on the level of 2007 with about one fifth population exposure in exceedance. Several countries with hardly any or no exceedances in 2007, do show in 2008 elevated PM_{10} annual averages well above the limit value. For example Cyprus with 87 %, caused by the one and only station reported and additionally with an annual average value being in 2008 well above the limit value and representing most of the Cypriot population. The 37 % in Greece was caused by a limited number of stations with elevated values at specifically urban stations. FYR of Macedonia (68 %), Serbia (62 %) and Montenegro (36 %) had a limited number of stations showing all rather elevated PM_{10} annual averages in 2008. Poland is on the same level as in 2007 with 12 % and Italy displays less then 3 % exposure above limit value. In a number of countries in north and north-western Europe, the LV of 40 $\mu g.m^{-3}$ seems not to be exceeded in continuation of previous years. When comparing 2008 with 2007, 2006 and 2005 we see that the population exposed to the low levels, i.e. below 20 $\mu g.m^{-3}$, has increased further to some 31 % after the temporary drop of 2006 to 20 % embedded in levels of 24 % in 2007 and 2005. The tendency of reducing population living above the limit value from 9 % in 2005, through 7.7 % in 2006 and 5.7 % in 2007, seems not to prolong in 2008 with its 5.8 %. Nevertheless, Jimmink et al. (2010) observes a slight decrease in the reported number of zones in exceedance to PM_{10} annual average, which may most likely conclude that an exposure reduction still develops in a positive direction despite some minor zone restructuring in 2008.

Considering the average for the whole of Europe, the overall population-weighted annual mean PM_{10} concentration is almost 25 $\mu g.m^{-3}$ and slightly lower than previous years: 1.5 $\mu g.m^{-3}$ lower than in 2005 (Horálek et al. 2008), 2.3 $\mu g.m^{-3}$ lower than in 2006 (De Smet et al. 2009) and 0.5 $\mu g.m^{-3}$ lower than in 2007 (De Smet et al. 2010). The slight decrease of the population-weighted concentration in comparison with 2007 and 2006 results is present in most EU countries with no limit value exceedance. The major exceptions are the countries with the highest exceedance levels; they show relative steep increases of population weighted concentrations.

Table 4.2 Population exposure and population weighted concentration – PM_{10}, annual average, year 2008. Resolution: 1x1 km.

Country		Population	2008 Percent [%]					Population weighted conc.
			< LV			> LV		
			< 10	10 - 20	20 - 40	40 - 45	> 45	
		x 1000	µg.m^{-3}	µg.m^{-3}	µg.m^{-3}	µg.m^{-3}	µg.m^{-3}	µg.m^{-3}
Austria	AL	8319	0.6	28.7	70.7	0	0	21.3
Belgium	BE	10667	0	5.2	94.8	0	0	23.9
Bulgaria	BG	7640	0	5.7	32.2	9.3	52.8	44.2
Croatia	HR	4436	0	1.4	98.6	0	0	28.1
Cyprus	CY	789	0	0	13	2	85	76.1
Czech Republic	CZ	10381	0	15.9	82.4	1.7	0	24.2
Denmark	DK	5476	0	76.3	23.7	0	0	18.8
Estonia	EE	1341	19.4	80.6	0	0	0	12.9
Finland	FI	5300	12.0	88.0	0	0	0	12.5
France	FR	64004	0	28.5	71.5	0	0	22.6
Germany	DE	82218	0	59.7	40.3	0	0	19.6
Greece	GR	11214	0	1.2	61.8	13.3	24	39.7
Hungary	HU	10045	0	2	98	0	0	26.8
Ireland	IE	4401	0.0	99.1	0.9	0	0	15.4
Italy	IT	59619	0.1	2.3	94.9	2.7	0.0	30.1
Latvia	LV	2271	0.3	36.1	63.6	0	0	19.1
Liechtenstein	LI	35	0	12.3	87.5	0	0	20.6
Lithuania	lt	3366	0	92.5	7.5	0	0	17.3
Luxembourg	LU	484	0	98.4	1.6	0	0	18.2
Malta	MT	410	0	0	100	0	0	27.5
Monaco	MC	32	0	0	100	0	0	29.5
Netherlands	NL	16405	0	0.2	99.8	0	0	24.0
Poland	PL	38116	0	15.1	72.5	7.4	5.0	28.3
Portugal	PT	10618	0.2	22.7	77.2	0	0	21.8
Romania	RO	21529	0	6.8	73.6	13.4	6.3	30.8
San Marino	SM	31	0	0	100	0	0	29.6
Slovakia	SK	5401	0	10.1	88.2	2	0	26.7
Slovenia	SI	2010	0	14.9	85.1	0	0	25.0
Spain	ES	45283	0.1	18.9	79.7	1.3	0	25.2
Sweden	SE	9183	3.3	90.4	6.3	0	0	16.3
United Kingdom	UK	61192	0.1	61.7	38.2	0	0	19.5
Albania	AL	3170	0	8.6	84.9	5	2	33.3
Andorra	AD	75	16.2	13	70.4	0	0	18.7
Bosnia-Herzegovina	BA	3844	0	9.4	90.6	0.0	0	29.3
Iceland	IS	315	4.2	95.8	0	0	0	15.2
Macedonia, F.Y.R. of	MK	2045	0	11.1	21.1	13.8	54.0	41.6
Montenegro	ME	628	0	19.3	42.0	36	2	33.6
Norway	NO	4737	14.0	82.9	3.1	0	0	15.7
Serbia (incl. Kosovo)	RS	9519	0	4.0	34.2	27.4	34.3	40.1
Switzerland	CH	7593	0.6	38.3	61.0	0	0	20.5
Total		**534144**	**0.4**	**30.9**	**63.0**	**2.7**	**3.0**	**24.8**
			31.3			**5.8**		

Note: In the lower pane countries for which the population numbers are based on ORNL population data with uncertain quality are AD, AL, BA, CH, IS, ME, MK, NO, RS. Turkey could not be included in the calculation due to lack of population density data.

4.1.3 Uncertainties

Uncertainty estimated by cross-validation

Using RMSE as the most common indicator, the *absolute mean uncertainty* of the combined final map at areas 'in between' the station measurements can be expressed in µg.m^{-3}. Table 4.1 shows that the absolute mean uncertainty of the combined final map of PM_{10} annual average expressed by RMSE is 5.0 µg.m^{-3} for the rural areas and 6.3 µg.m^{-3} for the urban areas. The result of this is that the map for 2007 shows the lowest evel of absolute mean uncertainties (4.6 and 5.0 µg.m^{-3}) compared to the maps of 2008, 2006 (5.8 and 6.1µg.m^{-3}) as well as 2005 (for both 5.5 µg.m^{-3}).

Alternatively, this uncertainty can be expressed in relative terms by relating the absolute RMSE uncertainty to the mean air pollution indicator value for all stations. This *relative mean uncertainty* of the combined final map of PM_{10} annual average 27.2 % for rural areas and 22.4 % for urban areas. This is higher than for the 2007 map (23.5 % and 18.4 %), the 2006 map (27 % and 21 %) and the 2005 map (25 % and 20 %). In urban areas the higher uncertainty compared to the previous years is caused specifically by Turkish urban background stations reported for the first time and thus used in the calculations for the first time (although interpolation result for Turkey is not presented in the map). These relative uncertainty values fulfil the data quality objectives for models as set in Annex I of the new air quality daughter directive EC (2008).

Figure 4.2 shows the cross-validation scatter plots, obtained according Section 2.3 of De Smet et al. (2010), for both the rural and urban areas. The R^2 indicates that for the rural areas about 48 % and for the urban areas about 82 % of the variability is attributable to the interpolation. Corresponding values of the map of 2005 (52 % and 71 %), 2006 (52 % and 69 %) and 2007 (59 % and 66 %), show for 2008 a reduced fit at the rural interpolations, but an improved fit for the urban interpolations.

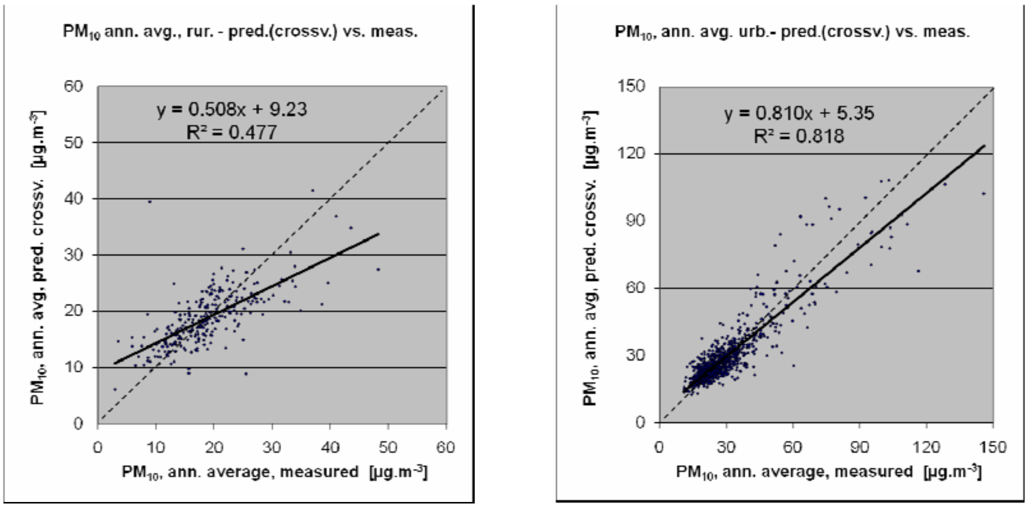

Figure 4.2 Correlation between cross-validation predicted values (y-axis) and measurements (x-axis) for the PM_{10} annual average for 2008 for rural (left) and urban (right) areas. R^2 and the slope a (from the linear regression equation $y = a \cdot x + c$) should be as close 1 as possible, the intercept c should be as close 0 as possible

The scatter plots indicate that in areas with high concentrations the interpolation methods tend to underestimate the levels. For example, in rural areas an observed value of 40 $\mu g.m^{-3}$ is estimated in the interpolations about 30 $\mu g.m^{-3}$, about 25 % too low. This underestimation at high values is natural to all spatial interpolations. It can be reduced by either using a higher number of the stations at improved spatial distribution, or introducing a closer regression by using other supplementary data.

Comparison of point measurement values with the predicted grid value

Additional to the above point observation - point prediction cross-validation, a simple comparison has been made between the point observation values and interpolated prediction values averaged in a 10x10 km^2 grid for the separate rural and urban map. This point-grid comparison indicates to what extent the predicted value of a grid cell represents the corresponding measured values at station(s) located in that cell. The results of the point observation - point prediction cross-validation of figure 4.2 compared to those of the point-grid validation are summarised in Table 4.3. The table shows a better correlated relation between (i.e. higher R^2, smaller intercept and slope closer to 1) station measurements and the interpolated values of the corresponding grid cells at both rural and urban map areas than it does at the point cross-validation predictions. That is because the simple comparison between point measurements and the gridded interpolated values shows the uncertainty at the actual station locations (points) itself, while the point observation – point prediction cross-validation simulates the behaviour of the interpolation at positions without actual measurements within the area covered by measurements. The uncertainty at measurement locations is caused partly by the smoothing effect of the interpolation and partly by the spatial averaging of the values in the 10x10 km^2 grid cells. The level of the smoothing effect leading to underestimation at areas with high values is there smaller than it is in case no measurement is present in such areas. For example, in urban areas the predicted interpolation gridded value will be about 47 $\mu g.m^{-3}$ at the corresponding station point with the measured value of 50 $\mu g.m^{-3}$, i.e. an underestimation of about 6 %.

Table 4.3 Linear regression equation and coefficient of determination R^2 from the scatter plots of (i) the predicted point values based on cross-validation and (ii) the aggregated predictions into 10x10 km^2 grid cells versus the measured point values for PM_{10} indicator annual average for rural and urban areas of 2008.

	rural areas		urban areas	
	equation	R^2	equation	R^2
i) cross-validation prediction (Fig4.2)	y = 0.508x + 9.23	0.477	y = 0.810x + 5.35	0.818
ii) 10x10 km grid prediction	y = 0.663x + 6.23	0.767	y = 0.866x + 3.65	0.914

Probability of Limit Value exceedance map

Next to the point cross-validation analysis we constructed a map with the probability of limit value exceedance. For this purpose, we aggregated the 1x1 km^2 gridded combined final concentration map into a 10x10 km^2 grid map. Then we derived with support of the 10x10 km^2 uncertainty map and the limit value (40 $\mu g.m^{-3}$) the probability of exceedance (PoE) map on a 10x10 km^2 grid resolution (Figure 4.3).

The map demonstrates areas with a probability of limit value exceedance above 75 % marked in red (*serious* probability) and areas below 25 % in green (*minor* probability). Red indicates areas for which exceedance may occur *very likely* due to either high concentrations close to or already above the LV accompanied with such uncertainty that exceedance is very likely, or areas with lower concentrations accompanied with high uncertainty levels reaching above the LV that excess is very likely. Vice versa, in the green areas it is *not likely* to have predicted concentrations and accompanying uncertainties at levels that do reach above the LV.

In the probability maps the areas with 25-50 %, resp. 50-75 % probability of LV exceedance are marked in yellow and orange. The yellow colour indicates the areas with the estimated concentrations below limit value, but for which there exist a *modest* probability of exceeding the limit. On the contrary, the orange areas have estimated concentrations above the limit value, but with a chance of non-exceedance caused by its accompanying uncertainty. Table 4.4 summarises the classes and terminology for probability (i.e. likelihood) that will be distinguished in this paper.

Table 4.4 Probability mapping classes and terminology use in this paper.

Map class colour	Percentage probability of threshold exceedance	Degree of probability (/ likelihood) of exceedance	Likelihood of exceedance
Green	0 – 25	Limited / Little	Not likely
Yellow	25 – 50	Modest	Somewhat likely
Orange	50 – 75	Moderate	Rather Likely
Red	75 – 100	Serious / Large	Very likely

The patterns in the spatial distribution of the different PoE classes over Europe differ in 2008 from those of 2005, 2006 and 2007. In the south-eastern Europe where relatively few measurement stations are located, Romania, Bulgaria, the Balkan countries and Greece show a further reduced probability of exceedance. Especially the capitals and larger agglomerations show clear reductions. The Albanian coastal zone, however, shows some increased probability of exceedance to levels of 20-50 %. Furthermore, Greece does show some increased PoE of 25-50 % (yellow) at the more densely populated areas (e.g. Athens, Thessaloniki and the cities on Crete). Most striking is the considerable increase of PoE for Cyprus coming from a low likelihood in 2007 to a modest to serious likelihood of exceedances at urbanised areas in 2008. The one station with high annual average observation values representing most population on Cyprus causes this jump. Contrary to that, the Iberian Peninsula shows in 2008 a further reduced PoE indicating little likelihood of exceedance for the whole area, which seems to indicate that 2006 was an exceptional year with elevated PoE.

In the other areas where exceedances are observed, such as the Po Valley and the south of Poland (Figure 4.1), the probability of exceedances are the highest and rather spatially extended, however at considerably lower levels than in 2007.

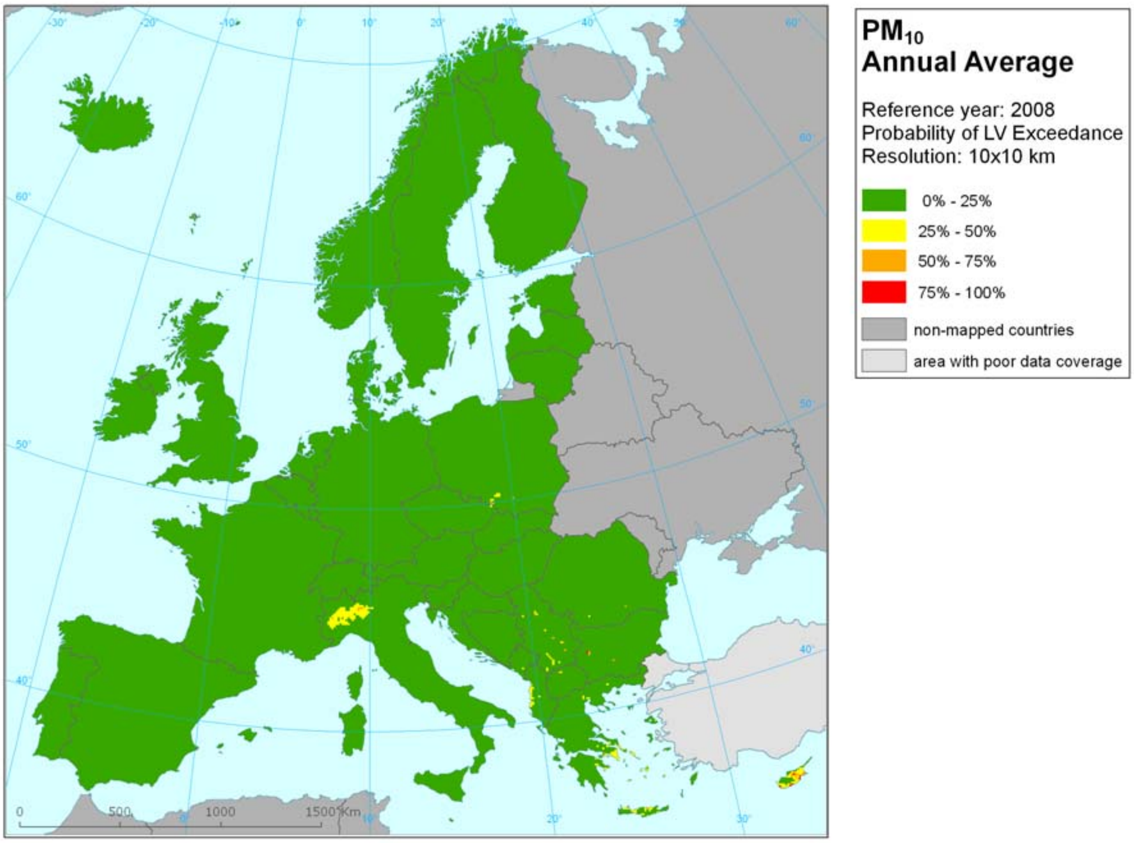

Figure 4.3 Map with the probability of the limit value exceedance for PM_{10} annual average ($\mu g.m^{-3}$) for 2008 on European scale calculated on10 x 10 km^2 grid resolution. Interpolation uncertainty is considered only (no other sources of uncertainty).

4.2 36th highest daily average

4.2.1 Concentration map

Similar to the PM_{10} annual average map, the combined final map of 36th highest daily values has been derived from the separate rural, urban and joint rural/urban maps, using the same set of supplementary data parameters (Section 4.1.1) in the regression and its residual interpolation. Table 4.5 presents the estimated parameters of the linear regression models and of the residual kriging, including its statistical indicators.

Table 4.5 Parameters of the linear regression models (Eq.2.1) and of the ordinary kriging variograms (nugget, sill, range) - and their statistics - of PM_{10} indicator 36^{th} maximum daily mean for 2008 in the rural (left) and urban (right) areas as used for final mapping, i.e. rural linear regression model P.Eawr (left), resp. urban UP.E (right), followed by the interpolation on its regression residuals using ordinary kriging (OK, coded with 'a').

linear regr. model + OK on its residuals	rural areas (lnP.Eawr-a)	urban areas (lnUP.E-a)
	coeff.	**coeff.**
c (constant)	2.92	3.76
a1 (lnEMEP model 2008)	0.263	n. sign.
a2 (altitude GTOPO)	-0.00048	
a3 (wind speed 2006)	-0.148	
a4 (s. solar radiation 2008)	0.040	
adjusted R^2	**0.26**	**0.00**
standard error [µg.m^{-3}]	**0.34**	**0.41**
nugget	0.04	0.02
sill	0.12	0.09
range [km]	600	330
RMSE [µg.m^{-3}]	**8.83**	**12.71**
MPE [µg.m^{-3}]	**0.26**	**0.00**

The regressions on the 2008 data have an adjusted R^2 of 0.26 for the rural areas and due to non-significance of the only supplementary data source; no regression is applied for the urban areas. This fit is worse than for 2007 (0.41, resp. 0.09) and back to the levels of years 2006 (0.27, resp. 0.02) and 2005 (0.29, resp. 0.06) (De Smet et al. 2010, 2009, Horálek et al. 2008). RMSE and MPE are the cross-validation indicators for the quality of the resulting map. Section 4.2.3 discusses in more detail the RMSE analysis and comparison with 2007, 2006 and 2005.

Figure 4.4 presents the combined final map, where areas and stations exceeding the limit value (LV) of 50 µg.m^{-3} on more than 35 days are coloured red and purple.

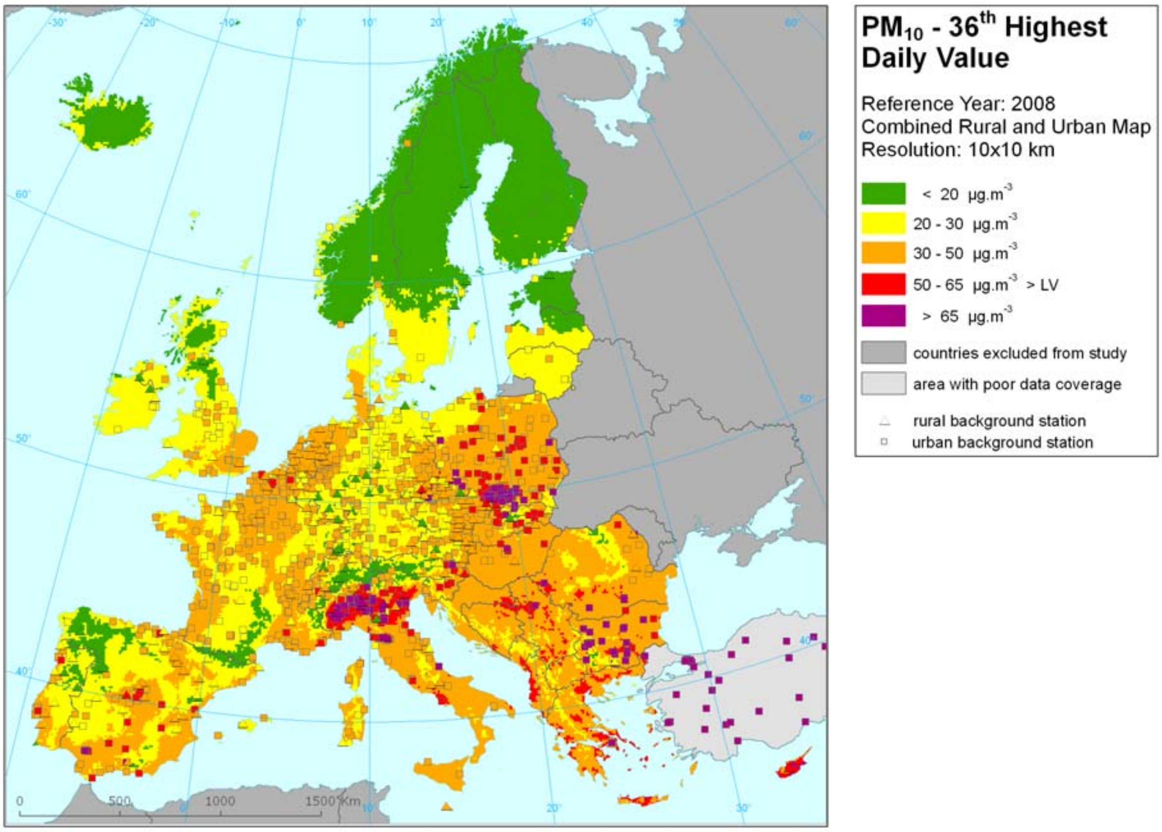

Figure 4.4 Combined rural and urban concentration map of PM_{10} – 36^{th} maximum daily average values, year 2008. Units: µg.m^{-3}. Resolution: 10x10 km.

4.2.2 Population exposure

Table 4.6 gives the population frequency distribution for a limited number of exposure classes calculated on a 1x1 km^2 grid resolution, as well as the population-weighted concentration for individual countries and for Europe as a whole. Shifted distributions are encountered in 2008 as opposed to previous years due to the increased merging resolution from now onward, as explained in Section 4.1.2.

Table 4.6 Population exposure and population weighted concentration – PM_{10}, 36^{th} maximum daily average value, year 2008. Resolution: 1x1 km.

Country		Population	2008 Percent [%]					Population-weighted conc.
			< LV			> LV		
			< 20	20 - 30	30 - 50	50 - 65	> 65	
		x 1000	$\mu g.m^{-3}$	$\mu g.m^{-3}$	$\mu g.m^{-3}$	$\mu g.m^{-3}$	$\mu g.m^{-3}$	$\mu g.m^{-3}$
Austria	AL	8319	0.9	12.3	86.8	0	0	36.9
Belgium	BE	10667	0	2.3	97.7	0	0	38.4
Bulgaria	BG	7640	0.0	1.5	23.1	11.5	63.9	78.2
Croatia	HR	4436	0	0.5	64.6	34.9	0.1	48.6
Cyprus	CY	789	0	0	1.7	11.9	86.4	130.7
Czech Republic	CZ	10381	0.1	6.2	80.6	7.0	6.1	42.5
Denmark	DK	5476	0.4	65.8	33.8	0	0	29.0
Estonia	EE	1341	29.1	69.3	1.6	0	0	22.4
Finland	FI	5300	32.9	67.1	0.0	0	0	21.9
France	FR	64004	0.5	12.6	86.3	0.6	0	36.3
Germany	DE	82218	0.3	23.0	76.7	0	0	31.7
Greece	GR	11214	0	0.4	14.7	48.5	36.4	64.9
Hungary	HU	10045	0	0.1	64.5	35.4	0	47.5
Ireland	IE	4401	0.5	96.8	2.7	0	0	25.8
Italy	IT	59619	0.1	0.7	53.0	28.7	17.5	51.7
Latvia	LV	2271	7.9	22.7	69.4	0	0	32.7
Liechtenstein	LI	35	0.226	1.1	98.6	0	0	38.5
Lithuania	LT	3366	0	45.0	55.0	0	0	29.5
Luxembourg	LU	484	0	64.6	35.4	0	0	29.1
Malta	MT	410	0	0	100.0	0	0	40.3
Monaco	MC	32	0	0	100.0	0	0	46.0
Netherlands	NL	16405	0	0.1	99.9	0	0	37.7
Poland	PL	38116	0.0	4.5	57.2	23.2	15.0	48.6
Portugal	PT	10618	2.4	15.6	81.9	0	0	35.5
Romania	RO	21529	0.1	2.2	44.3	30.0	23.4	53.1
San Marino	SM	31	0	0	74.1	25.9	0	48.9
Slovakia	SK	5401	0.1	5.2	56.5	32.0	6.2	47.5
Slovenia	SI	2010	0.0	6.0	88.5	5.5	0	42.7
Spain	ES	45283	1.6	10.7	75.2	10.7	1.9	40.1
Sweden	SE	9183	10.2	77.0	12.8	0	0	26.4
United Kingdom	UK	61192	0.6	23.5	76.0	0	0	32.1
Albania	AL	3170	0	4.1	19.3	65.2	11.4	55.7
Andorra	AD	75	19.6	9.4	71.0	0	0	29.3
Bosnia-Herzegovina	BA	3844	0	3.7	28.2	65.5	2.5	50.6
Iceland	IS	315	11.4	88.6	0.0	0	0	25.4
Macedonia, F.Y.R. of	MK	2045	0.0	3.4	22.7	5.2	68.6	71.5
Montenegro	ME	628	0	10.8	18.5	31.8	39.0	56.7
Norway	NO	4737	21.3	36.1	42.7	0	0	26.1
Serbia (incl. Kosovo)	RS	9519	0.0	1.0	21.5	12.4	65.1	68.6
Switzerland	CH	7593	1.1	10.5	86.5	1.9	0	36.5
Total		**516188**	**1.2**	**14.5**	**65.0**	**11.3**	**8.1**	**41.3**
			80.6			**19.4**		

Note: In the lower pane countries for which the population numbers are based on ORNL population data with uncertain quality are AD, AL, BA, CH, IS, ME, MK, NO, RS. Turkey could not be included in the calculation due to lack of population density data.

It has been estimated that in 2008 almost 20 % of the European population lived in areas where the 36th maximum daily mean of PM_{10} exceeds the limit value of 50 µg.m^{-3}. This is of about the same as in 2007. However, in Bulgaria, Cyprus, Greece, Romania, Albania, Bosnia-Herzegovina, FYR of Macedonia, Montenegro and Serbia both the populated weighted indicator concentration and the median were above the LV, implicating that in these countries the average concentration per inhabitant exceeded the LV and more than half of its population was exposed to concentrations exceeding the LV. Like in 2007, Italy has again a population weighted concentration above the LV, but its median dropped below the LV to 46 % of the population. In San Marino no longer the complete population lived in areas with concentrations above the LV; it dropped considerably to approximately 26 %. As the interpolation methodology tends to underestimate high values, these numbers will most likely be higher. The percentage of the total European population living in areas above the LV is 19.4 %, and reduced in 2008 with just 2.6 % compared to that of 2007 (22.0 %) and with about 9 % for 2006 (28.5 %) and 2005 (28.1 %).

Such reduction is less obvious at the overall European population-weighted concentration of the 36th maximum daily mean, which is estimated for the year 2008 at about 41 µg.m^{-3}. That is about 2.5 µg.m^{-3} lower than in 2005 (Horálek et al. 2008), about 4 µg.m^{-3} lower than in 2006 (De Smet et al. 2009) and just 1 µg.m^{-3} lower than in 2007 (De Smet et al. 2010). The further decrease of the population-weighted concentration in comparison with 2007 and 2006 results is present in many countries of the EU, including France that applies the PM correction factor by default now for the second year on row. The non-EU countries show an increase.

Comparing again the observed PM_{10} exceedances in 2008 for the indicator annual average (section 4.1.2) with 36th maximum daily average, like in 2007, one can conclude that the daily limit value is the most stringent of the two. Therefore, to comply with EU ambient air pollution legislation on PM10, countries best give preference to measures reducing PM10 concentrations to levels below the limit value for the 36th maximum daily mean.

4.2.3 Uncertainties

Uncertainty estimated by cross-validation

At first, the cross-validation analysis is performed. In Table 4.5 the absolute mean uncertainty of the combined map of PM_{10} indicator 36th highest daily mean for 2008 expressed by RMSE is 8.8 µg.m^{-3} for the rural areas and 12.7 µg.m^{-3} for the urban areas. For previous years the values were: 8.0 and 9.1 µg.m^{-3} in 2007, 13.3 and 9.9 µg.m^{-3} in 2006 and 9.8 and 11.7 µg.m^{-3} in 2005. It indicates that both rural and urban maps of 2007 show a lower absolute uncertainty than those of the 2008, 2006 and 2005 map.

The relative mean uncertainty (absolute RMSE relative to the mean indicator value) of the 2008 map of PM_{10} indicator 36th highest daily mean is 28.2 % for rural areas and 24.4 % for urban areas. The previous years had: 23.5 and 19.6 % in 2007, 26.3 and 21.4 % in 2006 and 26.6 and 23.5 % in 2005. In urban areas the higher uncertainty compared to the previous years is caused specifically by Turkish urban background stations reported for the first time in 2008 and as such used in the calculations for the first time (although interpolation result for Turkey is not presented in the map).

Figure 4.5 shows the cross-validation scatter plots for both rural and urban areas. The R^2 indicates that for the rural areas about 52 % and for the urban areas about 79 % of the variability is attributable to interpolation. Corresponding values with those of the 2005 map,55 % and 75 % respectively, the 2006 map, 56 % and 65 % resepectively, and 2007 map, 60 % and 65 % resepectively, show for 2008 a reduced fit for the rural areas, but an increased fit for the urban areas.

The scatter plots indicate that in areas with high concentrations the interpolation methods tend to underestimate the levels. For example, in urban areas (Figure 4.5, right panel) an observed value of 120 µg.m^{-3} would be estimated in the interpolation as about 100 µg.m^{-3}, i.e. about 17 % too low. For the rural areas it is even worse, but the predictions at the lower end of measurements suffer an overestimation at the rural areas which is not the case at the urban areas.

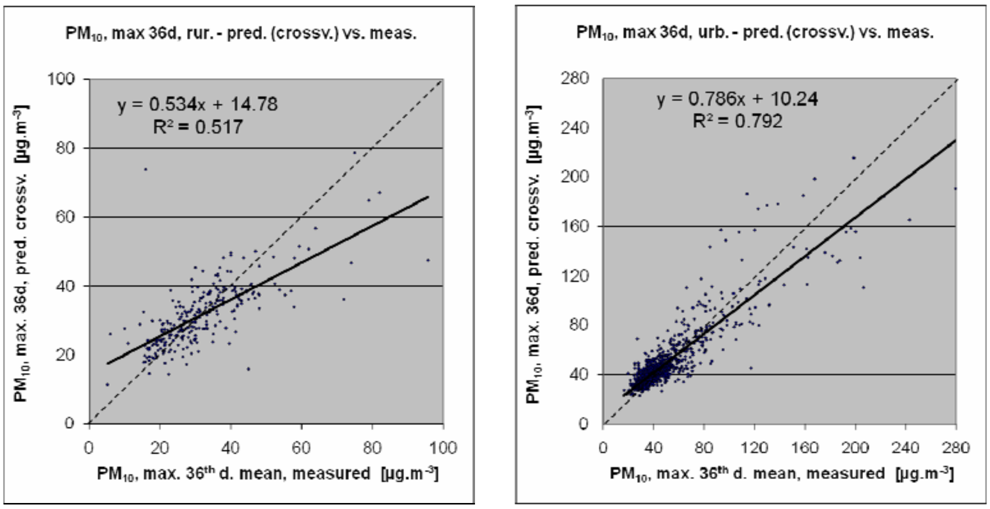

Figure 4.5 Correlation between cross-validation predicted values (y-axis) and measurements (x-axis) for the PM_{10} indicator 36th maximum daily mean for 2008 for rural (left) and urban (right) areas. R^2 and the slope a (from the linear regression equation y = a·x + c) should be as close 1 as possible, the intercept c should be as close 0 as possible.

Comparison of point measurement values with the predicted grid value

Additional to the point observation - point prediction cross-validation, a simple comparison has been made between the point observation values and interpolation predicted grid values. The results of the cross-validation compared to the gridded validation are summarised in Table 4.7. The uncertainty at measurement locations is caused partly by the smoothing effect of the interpolation and partly by the spatial averaging of the values in the 10x10 km^2 grid cells. The level of the smoothing effect leading to underestimation at areas with high values is at station locations smaller than it is in case no measurement is present in such areas. For example, in urban areas the predicted interpolation gridded value will be about 75 $\mu g.m^{-3}$ at the corresponding station point with the measurement value of 70 $\mu g.m^{-3}$, i.e. an underestimation of about 6 %.

Table 4.7 Linear regression equation and coefficient of determination R^2 from the scatter plots of (i) the predicted point values based on cross-validation and (ii) the aggregation into 10x10 km^2 grid cells versus the measured point values for PM_{10} indicator 36th maximum daily mean for rural and urban areas in 2008.

	rural areas		urban areas	
	equation	R^2	equation	R^2
i) cross-validation prediction (Fig 4.5)	y = 0.534x + 14.78	0.517	y = 0.786x + 10.24	0.792
ii) 10x10 km grid prediction	y = 0.688x + 9.72	0.809	y = 0.854x + 6.71	0.914

Probability of Limit Value exceedance map

Again we constructed the map with the probability of the limit value exceedance (PoE), using an aggregated 10x10 km^2 gridded concentration map (on the basis of the 1x1 km^2 combined final map of Figure 4.4), the 10x10 km^2 gridded uncertainty map and the limit value (LV, 50 $\mu g.m^{-3}$). Figure 4.6 presents the probability of exceedance 10x10 km^2 gridded map classifying the areas with probability of limit value exceedance below 25 % (limited PoE) in green, between 25-50 % (modest PoE) in yellow, between 50-75 % (moderate PoE) in orange and above 75 % in red (large PoE). Section 4.1.3 explains in more detail the significance of the colour classes in the map.

Comparing the probability of exceedance (PoE) of 2005, 2006 and 2007 with those of 2008, one can conclude that 2008 reveals throughout Europe a (further) reduction of both the extent of areas and the elevation of its levels of likelihood of exceedances. In many areas, these reductions consist of shifts to one lower PoE class. Several more local spots known as larger agglomerations and PM_{10} emitting

industrial areas, such as the Po Valley and the Black Triangle, showed also further reductions. In other words, one observes a considerably reduced likelihood of exceedances throughout Europe, except at some of the kernels of agglomerations and industrial regions where elevated PoE continue to exist. Most remarkable is the considerable reduction of the area with elevated PoE levels in the eastern part of the Po Valley and neighbouring relative densely populated regions. Nevertheless, in these areas considerable emission reductions may still be needed to reach non-exceedance levels in the future.
Where the Iberian Peninsula showed in 2006 and 2007 still areas with modest (yellow) and at the largest urbanised areas and agglomerations moderate (orange) to high (red) likelihood of exceedances, in 2008 these areas changed respectively into little (green) and modest (yellow) likelihood of exceedances. As an exception, Sevilla suffers still from a serious likelihood of exceedance (red), however over a less extended area. This could indicate that policy targets are or may be reached for the whole of Portugal and Spain in the near future. Keeping in mind that the interpolated maps refer to the rural or (sub)urban background situations only, it cannot be excluded that exceedances of the limit values may occur at many *hotspot* or traffic situations throughout Europe. Lowering of probabilities of exceedances from 2005 through 2008 are also observed in the Black Triangle, whereas the increase from 2005 to 2006 in the Benelux, Denmark, north-eastern Poland, Latvia, and Norway has diminished completely to levels below that of 2005. The same happens to the inner land of Greece, but to a less extent at the coastal zones in 2008 areas where modest (yellow) to moderate (orange) likelihoods are sustained at levels of 2007. The increases observed in 2006 in Hungary, Romania, Bulgaria, Balkan areas, east-coast of Italy, and some coastal zones of Greece, where the PoE had gone up from yellow to orange has been dropped again in 2007 and reached in 2008 levels below those of 2005. The PoE in the urbanised regions of Rome and Naples diminished also considerably in 2008. At Cyprus and to less extent at Crete the relatively high PoE have its cause in one or very few stations with measurements well above the limit value.

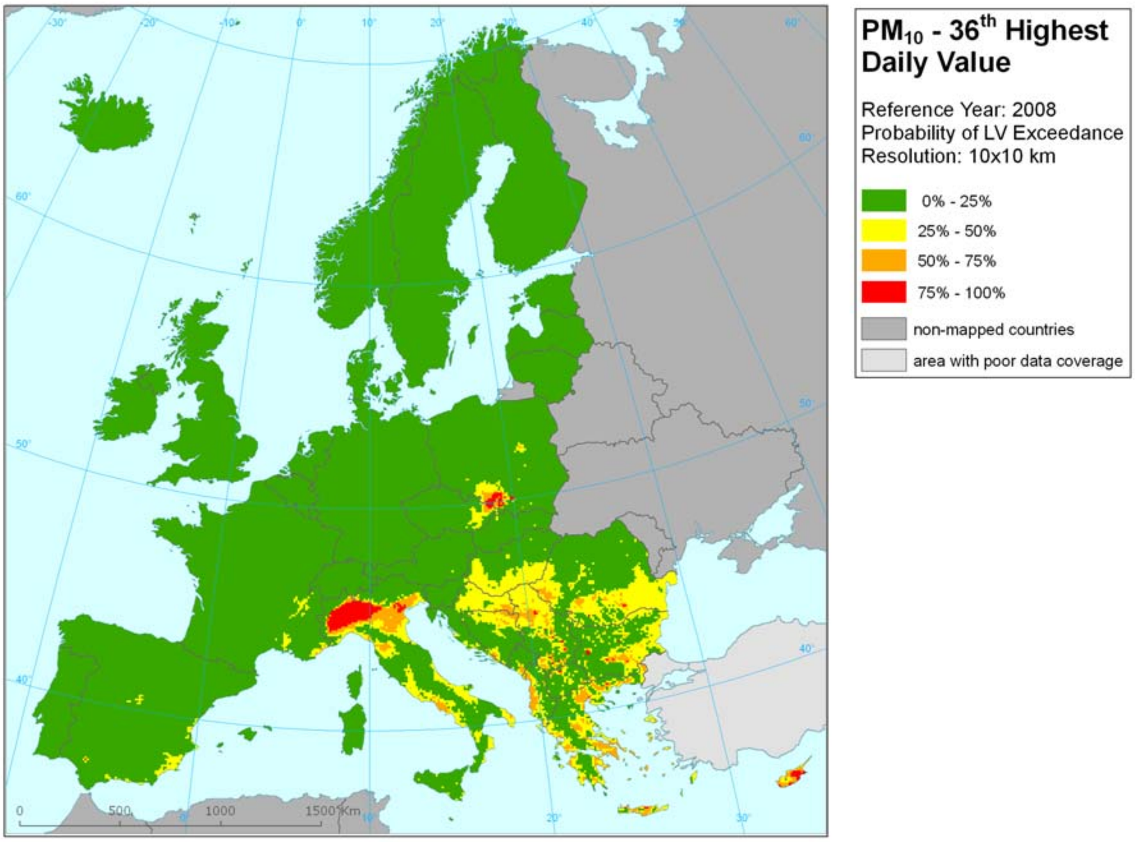

Figure 4.6 Map with the probability of the limit value exceedance for PM_{10} indicators 36^{th} maximum daily mean ($\mu g.m^{-3}$) for 2008 on the European scale calculated on the 10 x 10 km^2 grid resolution. Interpolation uncertainty is considered only (no other sources of uncertainty).

5 Ozone maps

For ozone, the two health-related indicators 26th highest daily maximum 8-hour running mean and SOMO35, and two vegetation-related indicators AOT40 for crops and the AOT40 for forests are considered. The maps with the health-related indicators are created using the combination of rural and urban areas on a 1x1 km^2 grid resolution, as described in Chapter 2, and presented in the EEA ETRS89-LAEA5210 projection on a 10x10 km^2 grid resolution. The maps of vegetation-related indicators are created for rural areas only and in a 2x2 km^2 grid covering the same mapping domain as for the human health indicators. This resolution serves the needs of the EEA Core Set Indicator 005 on ecosystem exposure to ozone.

5.1 26th highest daily maximum 8-hour average

5.1.1 Concentration map

Figure 5.1 presents the combined final map for 26th highest daily maximum 8-hour average as result of combining the separate rural and urban interpolated map following the procedures as described in more detail in De Smet et al. (2010) and Horálek et al. (2007). Both separate maps were created by combining the measured ozone concentrations with supplementary data in a linear regression model, followed by the interpolation of its residuals by ordinary kriging. The supplementary data used in the regression model for rural areas are EMEP model output, altitude and surface solar radiation for rural areas, and EMEP model output, wind speed and surface solar radiation for urban areas, respectively. (The relevant linear regression submodels have been identified earlier as O.Ear and UO.Ewr, respectively).

Table 5.1 presents the estimated parameters of the linear regression models and of the residual kriging, including the statistical indicators of both the regression and the kriging. The fit of the regression relation expressed as the adjusted R^2 is in 2008, with values of 0.41 for rural areas and 0.43 for urban areas, slightly poorer than in 2007 (0.51 and 0.48) and 2005 (0.45 and 0.51), but similar to 2006 (0.40 and 0.43) (De Smet et al. 2010 and 2009, Table 5.1; Horálek et al. 2008, Tables A3.1 and A3.11). The numbers show that over the years the fit of the regressions are reasonably of the same order of magnitude at both the rural and the urban areas. RMSE and MPE are the cross-validation indicators, showing the quality of the resulting map. Section 5.1.3 discusses in more detail the RMSE analysis and comparison with results of 2007, 2006 and 2005.

Table 5.1 Parameters of the linear regression models (Eq. 2.1) and of the ordinary kriging variograms (nugget, sill, range) - and their statistics - of ozone indicator 26th highest daily maximum 8-hour mean for 2008 in the rural (left) and urban (right) areas as used the for combined final map, i.e. linear regression model O.Ear (left), resp. UO.Ewr (right) followed by interpolation of its residuals using ordinary kriging (OK, coded 'a').

linear regr. model + OK on its residuals	**rural areas (O.Ear-a)**	**urban areas (UO.Ewr-a)**
	coeff.	**coeff.**
c (constant)	36.06	37.36
a1 (EMEP model 2008)	0.58	0.60
a2 (altitude GTOPO)	0.0056	
a3 (wind speed 2008)		-1.10
a4 (s. solar radiation 2008)	0.69	0.49
adjusted R^2	**0.41**	**0.43**
standard error [μg.m^{-3}]	**10.04**	**10.61**
nugget	63	40
sill	109	85
range [km]	490	80
RMSE [μg.m^{-3}]	**8.69**	**8.82**
MPE [μg.m^{-3}]	**0.02**	**0.05**

In the combined final map of Figure 5.1 the red and purple areas and stations do exceed the target value (TV) of 120 µg.m^{-3}. Note that in Directive 20008/50/EC the target value is defined as 120 µg/m3 not to be exceeded on more than 25 days per calendar year *averaged over three years*. Most likely, a three-year period has been set to reduce or eliminate largely the influence of annual meteorological variability. It would mean we should prepare the 76th highest daily maximum 8-hourly mean value for the period 2006-2008. However, this assessment specifically adresses the annual changes of air pollutants. Therefore, we calculate and prepare maps on annual basis.

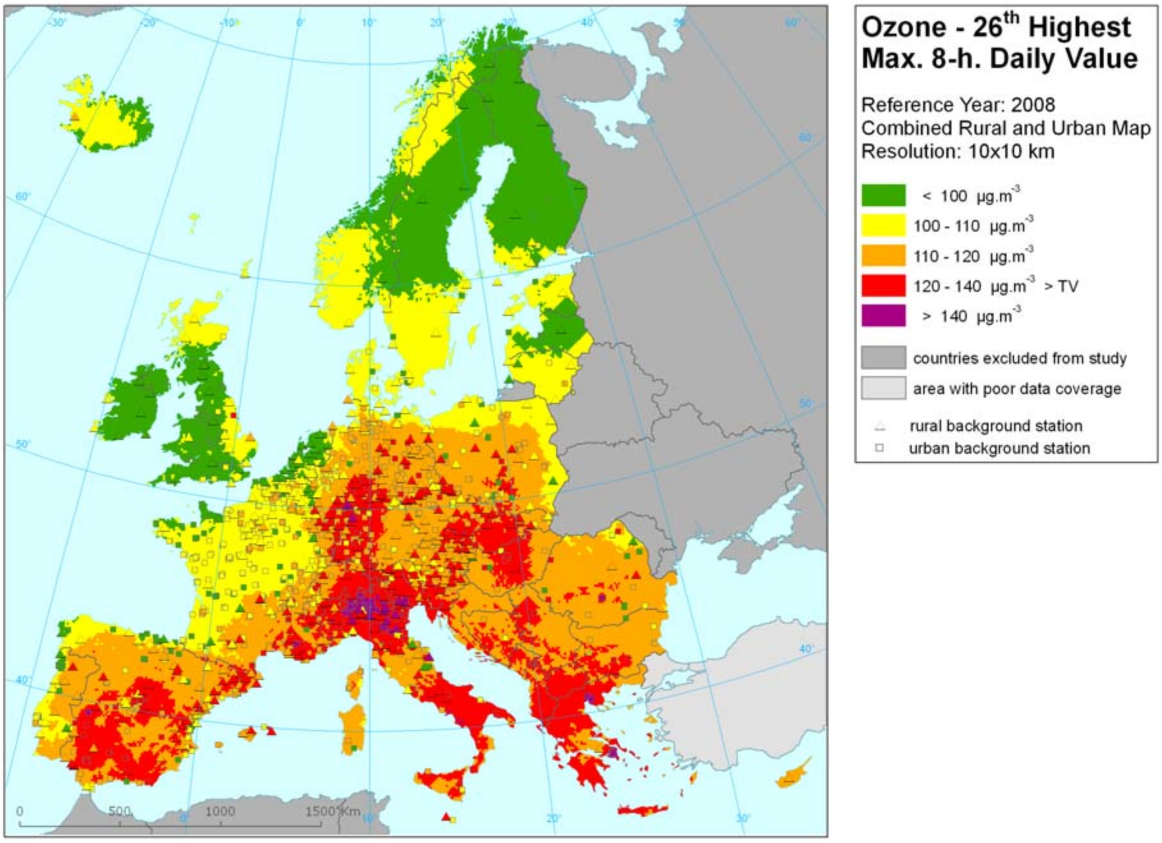

Figure 5.1 Combined rural and urban concentration map of ozone health indicators 26th highest daily maximum 8-hour value in µg.m^{-3} for the year 2008. Its target value is 120 µg.m^{-3}. Resolution: 10x10 km^2.

5.1.2 Population exposure

Table 5.2 gives for 26th highest daily maximum 8-hour mean the population frequency distribution for a limited number of exposure classes, as well as the population-weighted concentration for individual countries and for Europe as a whole. Be aware of shifted distributions in 2008 compared to previous years due to the increased merging resolution (from 10x10 km^2 grids to 1x1 km^2 grids), as explained in Section 4.1.2.

Table 5.2 Population exposure and population weighted concentration – ozone, 26th highest daily maximum 8-hour mean for the year 2008.

Country		Population x 1000	2008 Percent [%] < TV < 100 µg.m-3	2008 Percent [%] < TV 100 - 110 µg.m-3	2008 Percent [%] < TV 110 - 120 µg.m-3	2008 Percent [%] > TV 120 - 140 µg.m-3	2008 Percent [%] > TV > 140 µg.m-3	Population-weighted conc. µg.m-3
Austria	AL	8319	0	11.1	82.3	6.6	0	115.3
Belgium	BE	10667	11.4	87.9	0.6	0	0	103.6
Bulgaria	BG	7640	0	20.6	72.8	6.6	0	114.4
Croatia	HR	4436	0	10.2	81.0	8.8	0	115.5
Cyprus	CY	789	0	0.0	99.8	0.2	0	115.2
Czech Republic	CZ	10381	0	11.1	82.1	6.8	0	114.6
Denmark	DK	5476	34.7	65.3	0.0	0	0	102.6
Estonia	EE	1341	80.6	19.4	0	0	0	96.3
Finland	FI	5300	94.0	6.0	0	0	0	94.3
France	FR	64004	8.4	62.7	23.4	5.6	0	107.3
Germany	DE	82218	0.5	28.4	60.5	10.6	0	113.5
Greece	GR	11214	0	0	15.5	48.2	36.3	131.1
Hungary	HU	10045	0	0.3	71.0	28.6	0	117.5
Ireland	IE	4401	98.8	1.2	0	0	0	92.1
Italy	IT	59619	1.0	9.3	34.5	48.8	6.4	123.2
Latvia	LV	2271	90.9	9.1	0	0	0	94.9
Liechtenstein	LI	35	0	0	90.6	9.4	0	119.4
Lithuania	LV	3366	9.9	90.1	0	0	0	102.0
Luxembourg	LU	484	0.0	5.5	94.5	0	0	112.1
Malta	MT	410	0	90.2	8.2	1.6	0	108.4
Monaco	MC	32	0	0	0	100.0	0	123.1
Netherlands	NL	16405	65.0	35.0	0	0	0	98.4
Poland	PL	38116	2.9	53.1	42.2	1.9	0	109.7
Portugal	PT	10618	37.3	43.3	19.4	0.0	0	102.7
Romania	RO	21529	7.6	36.3	53.1	3.1	0	110.1
San Marino	SM	31	0	0	85.9	14.1	0	119.0
Slovakia	SK	5401	0	5.9	70.1	24.0	0	116.4
Slovenia	SI	2010	0	1.5	75.8	22.7	0	116.9
Spain	ES	45283	15.8	29.4	38.0	16.8	0	110.7
Sweden	SE	9183	68.7	31.3	0	0	0	97.6
United Kingdom	UK	61192	95.2	4.8	0	0	0	93.1
Albania	AL	3170	0	0	21.8	78.2	0	122.0
Andorra	AD	75	0	0	86.3	13.7	0	114.8
Bosnia-Herzegovina	BA	3844	0	28.0	64.5	7.5	0	113.7
Iceland	IS	315	85.7	14.3	0	0	0	90.8
Macedonia, F.Y.R. of	MK	2045	0	0	21.6	78.4	0	121.0
Montenegro	ME	628	0	0	87.7	12.3	0	118.1
Norway	NO	4737	67.2	32.8	0	0	0	99.0
Serbia (incl. Kosovo)	RS	9519	0	0.0	79.8	20.2	0	117.3
Switzerland	CH	7593	0	5.6	83.3	9.1	2.0	116.8
Total		**534144**	**21.2**	**27.8**	**35.9**	**13.4**	**1.6**	**109.8**
			85.0			**15.0**		

Note: In the lower pane countries for which the population numbers are based on ORNL population data with uncertain quality are AD, AL, BA, CH, IS, ME, MK, NO, RS. Turkey could not be included in the calculation due to lack of air quality or population density data.

It has been estimated that in 2008 some 15 % of the European population lived in areas where the ozone concentration exceeded the target value (TV of 120 µg.m^{-3}) of the 26th highest daily maximum 8-hour mean. This is a large reduction of more than a half compared to 2007 (34 %). All European countries do show a reduction in the number of population living in exceedance of the TV, expect for FYR of Macedonia where a serious increase is observed with about 34 % (from 44 % to 78 %). This somewhat deviating increase could likely have its cause in the limited number of observations with high values above TV representing, as such, a relative large number of Macedonian inhabitants.

Only the average concentration per inhabitant (i.e. population weighted concentration) of Greece, Italy, Monaco, Albania and FYR of Macedonia is estimated to be above the TV (like in 2007), with about 85 % of the Greek population, some 55 % of the Italians, all citizens of Monaco and about 78 % of the Albanians and Macedonians were exposed to level above the TV. Part of the population in Italy and Switzerland and more substantially in Greece (some 36 %) was exposed to ozone levels of even above the 140 µg.m^{-3}. As the current mapping methodology tends to underestimate high values, the numbers will most likely be higher. The Iberian Peninsula shows for 2008, compared to 2007, a reduction in exposure levels over the full range of 100 – 140 µg.m^{-3}. Many countries that had a population weighted concentration above the TV in 2007, do show in 2008 values just below the TV. European countries that had in 2007 most of their population exposed to (just) the lowest concentration class do show some increased exposure to higher concentrations up to 110 µg.m^{-3}, for example the Scandinavian and Baltic countries, the Netherlands, Belgium, UK, Ireland and Iceland. Most countries with population exposed to concentration levels above the TV in 2007 do show in 2008 a considerable reduction in population numbers exposed to exceedance. Many of these countries had in 2007 a population weighted concentration above the TV and show in 2008 values just under the TV, in the range of 114 – 119 µg.m^{-3}, for example, Austria, Bulgaria, Hungary, Slovakia and Slovenia, all, countries with a reasonable number of measurement stations. Nevertheless, the decrease in population weighted concentrations can be partially attributed to the higher resolution of the merger as described in Chapter 2.

We observe in 2008 a considerable further decrease in population exposed (reaching 15 %) to the higher ozone levels above the TV, compared to 2007 (34 %), 2006 (55 %) and 2005 (38 %). In general, the frequency distribution shows for 2008 a shift to increased percentages at indicator levels between 100 - 110 µg.m^{-3} and specifically 110 - and 120 µg.m^{-3} compared to 2007. This shift is both upward for most northern and north-western European countries and downward for most other European countries.

The overall European population-weighted ozone concentration in terms of the 26th highest daily maximum 8-hour mean is estimated for the year 2008 as 110 µg.m^{-3}. That is a decrease compared to previous years.

5.1.3 Uncertainties

Uncertainty estimated by cross-validation

The basic uncertainty analysis is given by cross-validation. Table 5.1 shows RMSE values of 8.7 µg.m^{-3} for the rural areas and 8.8 µg.m^{-3} for the urban areas of the combined final map. For previous years the values were for rural and urban areas respectively: 8.8 and 8.9 µg.m^{-3} (2007), 11.2 and 10.2 µg.m^{-3} (2006) and 12.3 and 10.0 µg.m^{-3} (2005). (De Smet et al. 2010 and 2009, Table 5.1; Horálek et al. 2008, Tables A3.3, A3.12). It indicates that the 2008 map has about the same absolute mean uncertainty at both the rural and urban areas compared to the 2007 and lower compared to the 2005 and 2006 map.

The relative mean uncertainty of the 2008 ozone map is 7.6 % for rural areas and 7.9 % for urban areas. The previous years had for rural and urban areas respectively: 7.5 % and 7.9 % (2007), 8.9% and 8.4 % (2006) and 10.3 % and 8.9 % (2005).

Figure 5.2 shows the cross-validation scatter plots for both the rural and urban areas of the 2008 map. The R^2, an indicator for the interpolation correlation with the observations, shows that for the rural areas about 56 % and, for the urban areas about 61 % of the variability is attributable to the interpolation. Corresponding values for the 2007 map (71 % and 66%), the 2006 map (49 % and 53 %) and the 2005 map (51 % and 50 %), show a fit at both the rural and urban interpolations that is better than in the 2005 and 2006 maps, but not as good as in the 2007 map.

The scatter plots indicate that the higher values are underestimated and the lower values somewhat overestimated by the interpolation method; a typical smoothing effect inherent to the linear regression and residual kriging interpolation method. For example, in rural areas (Figure 5.2, left panel) an observed value of 150 µg.m^{-3} is estimated in the interpolation as 135 µg.m^{-3}, which is 10 % too low.

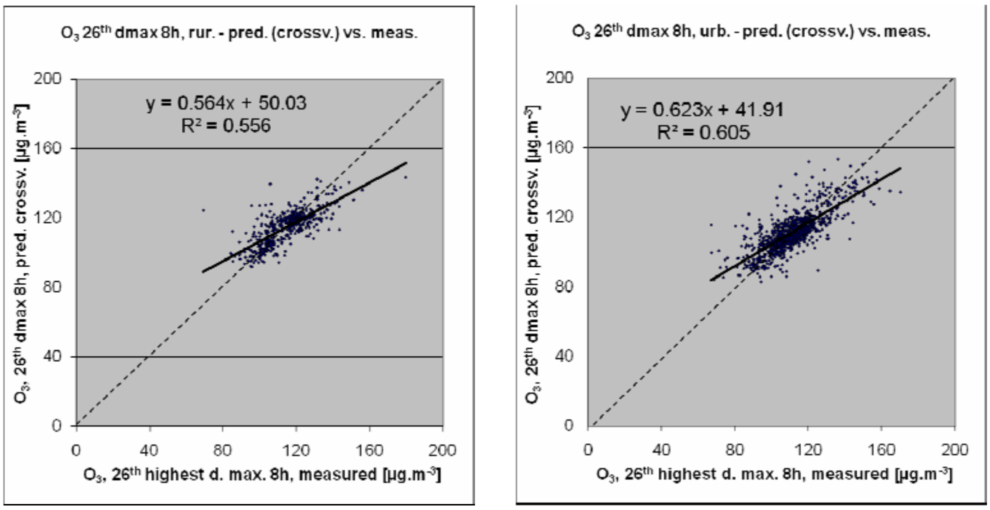

Figure 5.2 Correlation between cross-validation predicted values (y-axis) and measurements (x-axis) for the ozone indicator 26th highest daily maximum 8-hour mean for rural (left) and urban (right) areas in 2008.

Comparison of point measurement values with the predicted grid value

Additional to the point observation - point prediction cross-validation, a simple comparison has been made between the point observation values and interpolated predicted grid values. The results of the cross-validation compared to the gridded validation examination are summarised in Table 5.3. The uncertainty at measurement locations is caused partly by the smoothing effect of interpolation and partly by the spatial averaging of the values in the 10x10 km^2 grid cells. The level of smoothing leading to underestimation at areas with high values is here smaller in case no measurement is present in such areas. For example, in rural areas the predicted interpolation grid value will be about 130 µg.m^{-3} at the corresponding station point with the observed value of 140 µg.m^{-3}, i.e. an underestimation of about 9 %.

Table 5.3 Linear regression equation and coefficient of determination R^2 from the scatter plots of (i) the predicted point values based on cross-validation and (ii) aggregation into 10x10 km^2 grid cells versus the measured point values for the ozone indicator 26th highest daily maximum 8-hour mean for rural and urban areas of 2008.

	rural areas		urban areas	
	equation	R^2	equation	R^2
i) cross-validation prediction (Fig 5.2)	y = 0.564x + 50.03	0.556	y = 0.623x + 41.91	0.605
ii) 10x10 km grid prediction	y = 0.651x + 40.05	0.726	y = 0.768x + 25.90	0.850

Probability of Target Value exceedance map

A 10x10 km^2 gridded map with the probability of the target value exceedance in Figure 5.3 has been constructed on basis of the 10x10 km^2 gridded concentration map (Figure 5.1) as aggregation of the 1x1 km^2 gridded map, the 10x10 km^2 gridded uncertainty map and the target value (TV) of 120 µg.m^{-3}. Section 4.1.3 explains in more details the significance of the classes in the map.

Comparing 2008 with 2007 – 2005 it becomes evident that after the year 2006 with its temporal increase in PoE to levels above 50 % and even above 75 % in large parts of specifically central Europe, a continued and well-observed decrease took place in the levels of PoE in 2007 and 2008, to levels in many areas well below those of 2005. In 2008, most of the red areas (serious PoE) turned into orange (moderate PoE) and even yellow (modest PoE), except for the northern and more southern regions of Italy, parts of Greece, inner Spain and the more south-western Germany region, where they show unchanged elevated likelihood of exceedances (red, > 75 %). Most of the orange zones in 2007 turned yellow in 2008; a few became green (central Italy and Romania, North-West Iberian Peninsula). Remarkable is the increased probability of exceedance observed in south-western Spain, especially around its larger cities. The somewhat elevelated PoE in 2007 in the eastern part (South Poland, Slovakia, Hungary, Balkan region) has disappeared largely to some moderate PoE levels (orange) in West Slovakia, central Hungary and the southern Balkan. The other areas have just a modest PoE (yellow). In the south-east of Europe the increase of 2007 has diminished again to levels of 2006 and even below.

The meteorologically induced variations from year to year, combined with methodological uncertainties and the limited number of years considered here do not allow for conclusions on any significant tendency. For that purpose, one would need longer time series and reduced uncertainties.

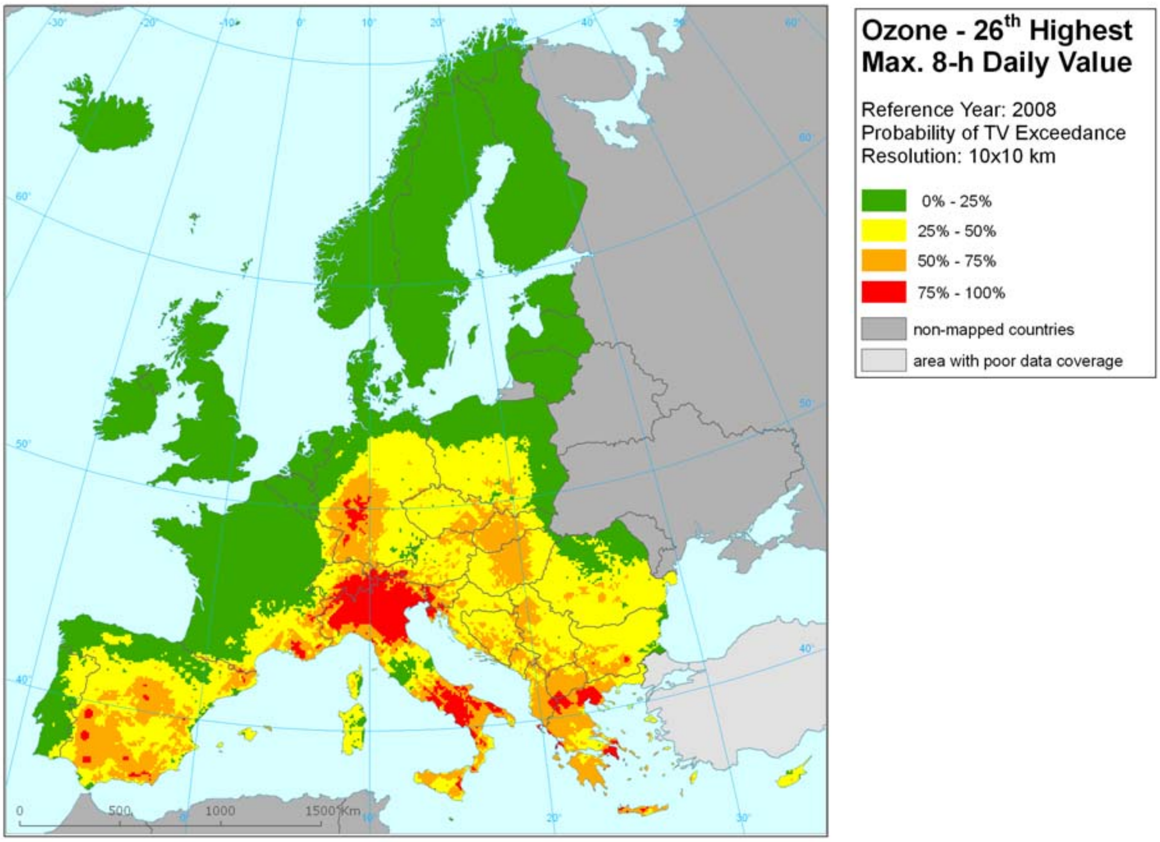

Figure 5.3 Map with the probability of the target value exceedance for ozone indicator 26th highest daily maximum 8-hour average (µg.m^{-3}) for 2008 on European scale calculated on the 10 x 10 km^2 grid resolution. Interpolation uncertainty is considered only(no other sources of uncertainty).

5.2 SOMO35

5.2.1 Concentration map

Figure 5.4 presents the combined final map for SOMO35 as result of combining the separate rural and urban interpolated map following the procedure as described in De Smet et al. (2010) and Horálek et al. (2007).

The supplementary data used in the regression models are the same as for 26th highest daily maximum 8-hour mean, i.e. EMEP model output, altitude and surface solar radiation for rural areas and EMEP model output, wind speed and surface solar radiation for urban areas. (The relevant linear regression submodels are identified as O.Ear, resp. UO.Ewr.)

Table 5.4 presents the estimated parameters of the linear regression models and of the residual kriging, including the statistical indicators of both the regression and the kriging. The fit of the regression is expressed by the adjusted R^2 and standard error. The adjusted R^2 is in 2008 for the rural areas 0.49 and for the urban areas 0.44, and as such a somewhat poorer fit than in 2007 (both 0.58) and 2005 (0.51 and 0.49) but slightly better than in 2006 (0.42 and 0.38) (De Smet et al. 2010 and 2009, Table 5.4; Horálek et al. 2008, Tables A3.1 and A3.11). RMSE and MPE are the cross-validation indicators showing the quality of the resulting map. Section 5.2.3 discusses in more detail the RMSE analysis and comparison with results of 2007, 2006 and 2005.

Table 5.4 Parameters of the linear regression models (Eq. 2.1) and of the ordinary kriging variograms (nugget, sill, range) - and their statistics - of ozone indicator SOMO35 for 2008 in the rural (left) and urban (right) areas as used for final mapping, i.e. rural linear regression model O.Ear (left), resp. UO.Ewr (right) followed by the interpolation on its residuals using ordinary kriging (OK, coded with ‘a’).

linear regr. model + OK on its residuals	**rural areas (O.Ear-a)**	**urban areas (UO.Ewr-a)**
	coeff.	**coeff.**
c (constant)	-390	-999
a1 (EMEP model 2008)	0.41	0.43
a2 (altitude GTOPO)	1.50	
a3 (wind speed 2008)		n. sign.
a4 (s. solar radiation 2007)	190.24	177.12
adjusted R^2	**0.49**	**0.44**
standard error [μg.m^{-3}.d]	**1702**	**1507**
nugget	2.1E+06	7.0E+05
sill	2.2E+06	1.5E+06
range [km]	500	80
RMSE [μg.m^{-3}.d]	**1609**	**1293**
MPE [μg.m^{-3}.d]	**-15**	**-1**

SOMO35 is not subject to one of the EU air quality directives and no limit or target values have been defined, which does not offer the possibility to create a map with the probability of exceedances.

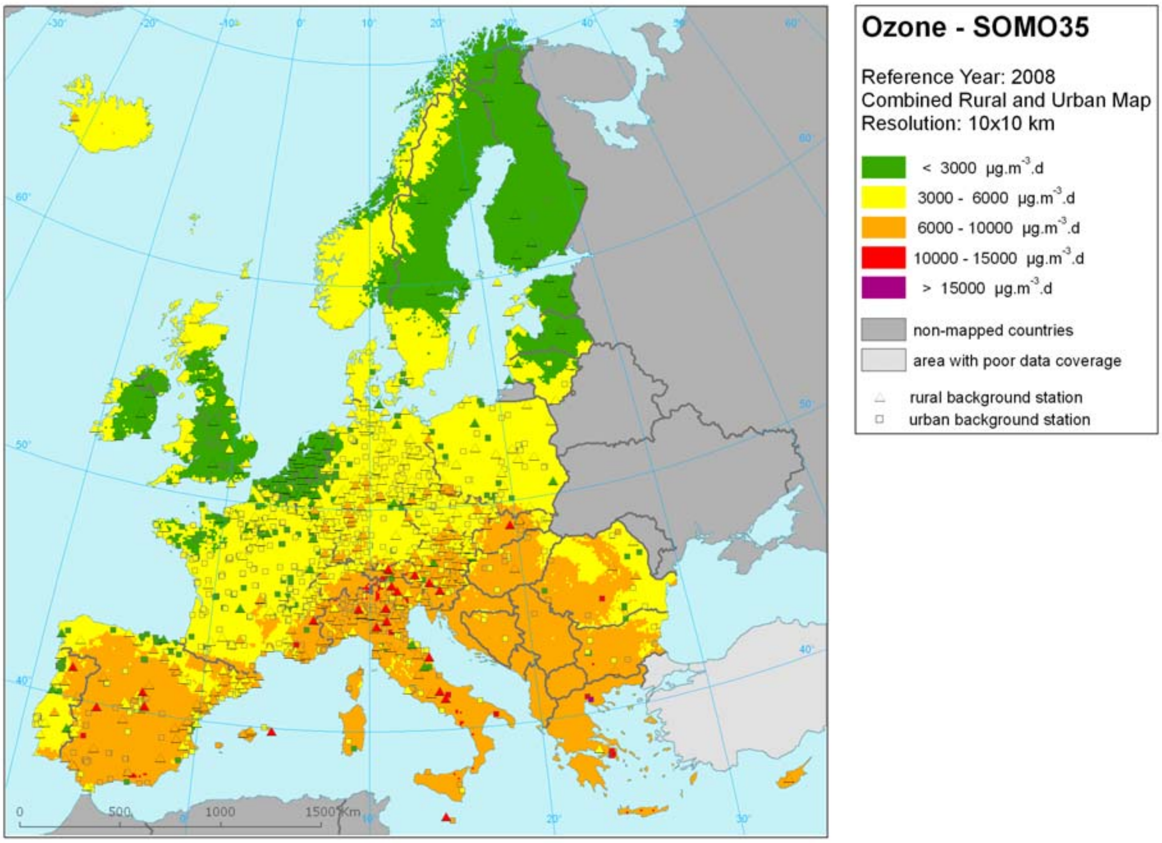

Figure 5.4 Combined rural and urban concentration map of ozone indicators SOMO35 in µg.m^{-3}.days for the year 2008. Resolution: 10x10 km^2.

5.2.2 Population exposure

Table 5.5 gives for SOMO35 the population frequency distribution for a limited number of exposure classes, as well as the population-weighted concentration for individual countries and for Europe as a whole. Again, shifted distributions occur in 2008 compared to previous years due to the increased merging resolution (from 10x10 km^2 grids to 1x1 km^2 grids) as explained in Section 4.1.2.

It has been estimated that in 2008 almost 20 % of the European population lived in areas with SOMO35 values above 6000 µg.m^{-3}.d. This is a reduction compared to 2007 (33 %), 2006 (37 %) and 2005 (34 %). All European countries do show a reduction in the number of people living in 2008 in areas submitted to more than 6000 µg.m^{-3}.d, except for Greece where an increase is observed of about 20 % (from 16 % to 36 %). Comparing the national frequency distribution of 2008 with that of 2007, one observes a slight overall shift from the higher classes and also from its lower class interval to the interval 3000 – 6000 µg.m^{-3}.d. These shifts can be observed in the maps as well: an expansion of the yellow areas in 2008 at expenses of both the green and orange areas in 2007. For example, many central European and Balkan countries do show reductions from levels well above, to levels below the 6 000 µg.m^{-3}.d. Furthermore, the reduction of population exposed to levels above 10 000 µg.m^{-3}.d in 2008 can be observed in the maps: almost all the red areas (above 10 000 µg.m^{-3}.d) in the 2007 map have diminished completely and turned into orange in the 2008 map, except for the Greek area around Athens and a few grid cells in relative low populated rural areas of Austria, Bulgaria, Czech Republic, Italy, Spain and Switzerland. Most countries that do show a shift in exposures from the lowest class interval to its neighbouring higher interval are situated mainly in northern and north-western Europe, for example France, Germany, Ireland, the Scandinavian and Baltic states. The Iberian Peninsula shows compared to previous years, a considerable further reduced population exposure with a magnitude of several class intervals.

The total European population-weighted ozone concentration in terms of SOMO35 was estimated as 4275 $\mu g.m^{-3}.d$ and is a further decrease compared to the previous years 2007, 2006 and 2005.

Table 5.5 Population exposure and population weighted concentration – ozone, SOMO35, year 2008.

Country		Population x1000	2008 Percent [%] < 3000 µg.m-3.d	3000 - 6000 µg.m-3.d	6000 - 10000 µg.m-3.d	10000 - 15000 µg.m-3.d	> 15000 µg.m-3.d	Population-weighted conc. µg.m-3.d
Austria	AL	8271	0	87.5	12.5	0	0	5099
Belgium	BE	10579	95.4	4.6	0	0	0	2520
Bulgaria	BG	7982	0	52.3	47.7	0	0	5797
Croatia	HR	4464	0	64.2	35.8	0	0	5899
Cyprus	CY	852	0	0	100	0	0	8027
Czech Republic	CZ	10164	0	98.3	1.7	0	0	4576
Denmark	DK	5415	51.1	48.9	0	0	0	3080
Estonia	EE	1335	96.6	3.4	0	0	0	2363
Finland	FI	5129	99.0	1.0	0	0	0	1938
France	FR	58495	35.6	59.8	4.7	0	0	3563
Germany	DE	82111	18.5	81.0	0.5	0	0	3822
Greece	GR	10967	0	0.1	63.9	36.0	0	8969
Hungary	HU	10128	0	74.5	25.5	0	0	5751
Ireland	IE	3730	90.4	9.6	0	0	0	2096
Italy	IT	56794	0.0	33.8	66.1	0	0	6386
Latvia	LV	2383	90.2	9.8	0	0	0	2347
Liechtenstein	LI	67	0	93.6	6.4	0	0	4930
Lithuania	LT	3469	40.1	59.9	0	0	0	3059
Luxembourg	LU	425	0.1	99.9	0	0	0	3557
Malta	MT	395	0	0	100	0	0	6582
Monaco	MC	32	0	0	100	0	0	7246
Netherlands	NL	15729	99.5	0.5	0	0	0	2104
Poland	PL	38223	6.4	93.0	0.7	0	0	3951
Portugal	PT	9906	27.1	64.4	8.6	0	0	3851
Romania	RO	22428	6.9	75.2	17.9	0	0	5039
San Marino	SM	20	0	85.9	14.1	0	0	5863
Slovakia	SK	5298	0	80.5	19.5	0	0	5455
Slovenia	SI	2030	0	62.8	37.2	0	0	5761
Spain	ES	38992	12.6	54.8	32.6	0	0	5110
Sweden	SE	8887	84.3	15.7	0	0	0	2387
United Kingdom	UK	59029	95.2	4.8	0	0	0	2044
Albania	AL	3927	0	0	100	0	0	7668
Andorra	AD	61	0	70.4	29.6	0	0	6319
Bosnia-Herzegovina	BA	4175	0	62.6	37.4	0	0	5972
Iceland	IS	178	68.9	31.1	0	0	0	2224
Macedonia, F.Y.R. of	MK	2275	0	0	100	0	0	7133
Montenegro	ME	713	0	0	100	0	0	7120
Norway	NO	3187	81.1	18.9	0	0	0	2514
Serbia (incl. Kosovo)	RS	10736	0	25.1	74.9	0	0	6378
Switzerland	CH	7238	0	91.4	8.5	0.1	0	4619
Total		**516188**	**30.2**	**50.2**	**18.8**	**0.8**	**0.0**	**4275**
			80.4		**19.6**			

Note: In the lower pane countries for which the population numbers are based on ORNL population data with uncertain quality are give (AD, AL, BA, CH, IS, ME, MK, NO, RS). Turkey could not be included in the calculations due to lack of air quality or population density data.

5.2.3 Uncertainties

Uncertainty estimated by cross-validation

The basic uncertainty analysis is given by cross-validation. In Table 5.4 the absolute mean uncertainty (RMSE) in 2008 is 1609 µg.m^{-3}.d for the rural areas and 1293 µg.m^{-3}.d for the urban areas. This means a further improvement in uncertainty reduction compared to its previous years 2007 (1801 and 1260 µg.m^{-3}.d), 2006 (2077 and 1472 µg.m^{-3}.d) and 2005 (2173 and 1459 µg.m^{-3}.d).

The relative mean uncertainty of the 2008 map of SOMO35 is 30.7 % for rural areas and 31.3 % for urban areas. The previous years had for rural and urban areas respectively: 33.3 % and 29.5 % (2007), 31.6 % and 29.2 % (2006) and 35.5 % and 32 % (2005), meaning that the 2008 relative uncertainties are for rural areas at the lower end of the range and for urban well within the range of previous years' values.

Figure 5.5 shows the cross-validation scatter plots for interpolated values at both rural and urban areas. R^2 indicates that for the rural areas about 54 % and for the urban areas about 58 % of the variability is attributable to the interpolation. The corresponding values for the 2007 maps (63 % and 67 %), the 2006 maps (47 % and 49 %) and 2005 maps (55 % and 58 %), illustrate a somewhat similar fit at rural areas in 2008 and 2007 and a somewhat reduced fit at urban.

The scatter plots show again that in areas with high concentrations the interpolation methods tend to deliver underestimated predicted values, with additionally at the urban areas at the lower values some overestimation. For example, in urban areas (Figure 5.5, right panel) an observed value of 10 000 µg.m^{-3}.d is estimated in the interpolation as about 7500 µg.m^{-3}.d. That is 25 % too low, leading in general to high underestimations at high SOMO35 values. Vice versa at low values an overestimation will occur, e.g. at a measured 2000 µg.m^{-3}.d the interpolation will predict some 3000 µg.m^{-3}.d, which is about 50 % too high.

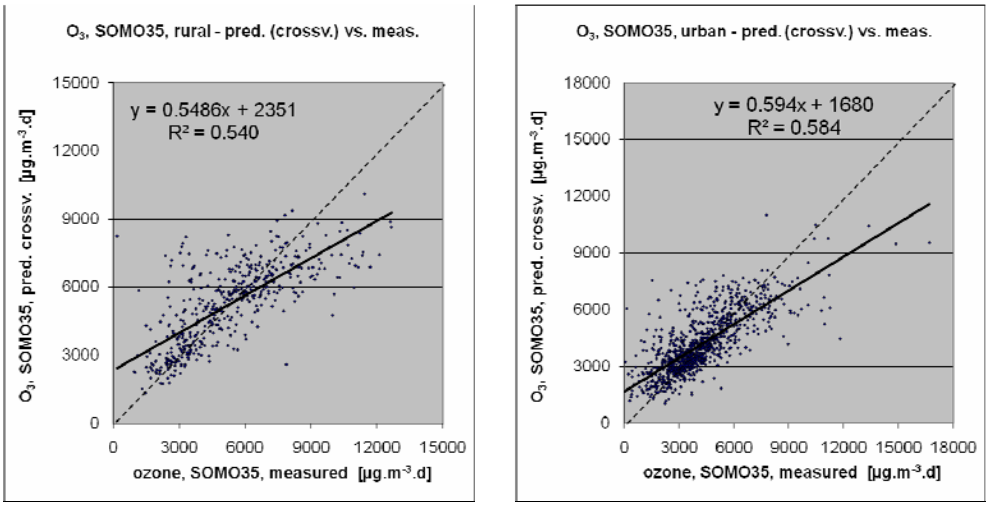

Figure 5.5 Correlation between cross-validation predicted values (y-axis) and measurements (x-axis) for the ozone indicator SOMO35 for rural (left) and urban (right) areas in 2008.

Comparison of point measurement values with the predicted grid value

Additional to the point observation - point prediction cross-validation, a simple comparison has been made between the point measurement and interpolated predicted grid values averaged in a 10x10 km grid for the separate rural and urban map. This point-grid comparison indicates to what extent the predicted value of a grid cell represents the corresponding measured values at stations located in that cell. The results of the point observation - point prediction cross-validation of Figure 5.5, compared to those of the point-grid validation are summarised in Table 5.6. The table shows a better correlated relation (i.e. higher R^2, smaller intercept and slope closer to 1) between station measurements and the interpolated values of the corresponding grid cells (case ii) at both rural and urban map areas than it does at the point cross-validation predictions (case i). That is because the simple comparison between point measurements and the gridded interpolated values shows the uncertainty at the actual station locations (points) itself, while the point observation – point prediction cross-validation simulates the behaviour of the interpolation at positions without actual measurements within the area covered by measurements. The uncertainty at measurement locations is caused partly by the smoothing effect of the interpolation and partly by the spatial averaging of the values in the 10x10 km^2 grid cells. The level of the smoothing effect leading to underestimation at areas with high values is there smaller than it is in case no measurement is present in such areas. For example, in urban areas the predicted interpolation grid value will be about 8600 µg.m^{-3}.d at the corresponding station point with the observed value of 10 000 µg.m^{-3}.d, i.e. an underestimation of about 14 %.

Table 5.6 Linear regression equation and coefficient of determination R^2 from the scatter plots of (i) the predicted point values based on cross-validation and (ii) aggregation into 10x10 km^2 grid cells versus the measured point values for the ozone indicator SOMO35 for rural and urban areas of 2008.

	rural areas		urban areas	
	equation	R^2	equation	R^2
i) cross-validation prediction (Fig 5.5)	y = 0.549x + 2351	0.540	y = 0.594x + 1680	0.584
ii) 10x10 km grid prediction	y = 0.609x + 2037	0.661	y = 0.753x + 1027	0.853

No Limit Value or Target Value is set for the WHO recommended ozone health indicator SOMO35, therefore no probability of exceedance map has been prepared.

5.3 AOT40 for crops and for forests

The ecosystem based accumulative ozone indicators described in this section are specifically intended for insertion in the EEA Core Set of Indicator 005 (CSI005, http://themes.eea.europa.eu/indicators). For the estimation of the vegetation and forest land areas exposures to accumulated ozone, the maps in this section are created on a 2x2 km^2 grid, instead the 10x10km^2 grid resolution used to calculate the separate rural and urban maps for the human health indicators. This resolution is selected as a compromise between calculation time and accuracy in the impact analysis done for the ozone impact assessment of the CSI005, which uses results of this section. It serves a refinement of the exposure frequency distribution outcomes of the overlay with the 100x100 m^2 resolution -CLC2000 land cover classes.

5.3.1 Concentration maps

The interpolated maps for AOT40 for crops and AOT40 for forests have been created for rural areas only, combining AOT40 data derived from rural background station observations with the supplementary data sources EMEP model output, altitude and surface solar radiation. (The relevant linear regression submodel is identified as O.Ear.). Note that supplementary data sources are the same as at the human health related ozone indicators.

Table 5.7 presents the estimated parameters of the linear regression models and of the residual kriging, including their statistical indicators of the regression and kriging. The fit of the regression is expressed by adjusted R^2 and the standard error. The adjusted R^2 is in 2008 for AOT40 for crops 0.49 and for AOT40 for forests 0.59, and as such about the poorest fit for both indicators, since these values are at the lower end of the range of values for the four consecutive years: 2007 (0.49 and 0.59), 2006 (0.45 and 0.47) and 2005 (0.53 and 0.52). (De Smet et al. 2010 and 2009, Table 5.7; Horálek et al. 2008, Table A3.2). RMSE and MPE are the cross-validation indicators, showing the quality of the resulting map. Section 5.2.3 discusses in more detail the RMSE analysis and comparison with results of 2007, 2006 and 2005.

Table 5.7 Parameters of the linear regression models (Eq2.1) and of the ordinary kriging variograms (nugget, sill, range) - and their statistics - of ozone indicators AOT40 for crops (left) and for forests (right) for 2008 in the rural areas as used for final mapping, i.e. rural linear regression model O.Ear followed by the interpolation on its residuals using ordinary kriging (OK, coded with 'a').

linear regr. model + OK on its residuals	AOT40 for crops (O.Ear-a)	AOT40 for forests (O.Ear-a)
	coeff.	coeff.
c (constant)	1563	-6123
a1 (EMEP model 2008)	0.41	0.39
a2 (altitude GTOPO)	3.58	6.20
a3 (s. solar radiation 2008)	383.1	1237.8
adjusted R^2	**0.40**	**0.49**
standard error [μg.m^{-3}]	**6008**	**9442**
nugget	2.0E+07	5.7E+07
sill	3.7E+07	8.6E+07
range [km]	450	470
RMSE [μg.m^{-3}]	**5283**	**8750**
MPE [μg.m^{-3}]	**24**	**-1**

Figure 5.6 presents the final map of AOT40 for crops. The areas and stations in the map that exceed the target value (TV) of 18 mg.m^{-3}.h are marked in red and purple. It concerns a map for rural areas, just based on rural background station observations, representing an indicator for vegetation exposure to ozone while assuming there is no relevant vegetation in the urban areas.

The same holds for the final rural map of AOT40 for forests as presented in Figure 5.7. However, for AOT40 for forests there is no TV defined.

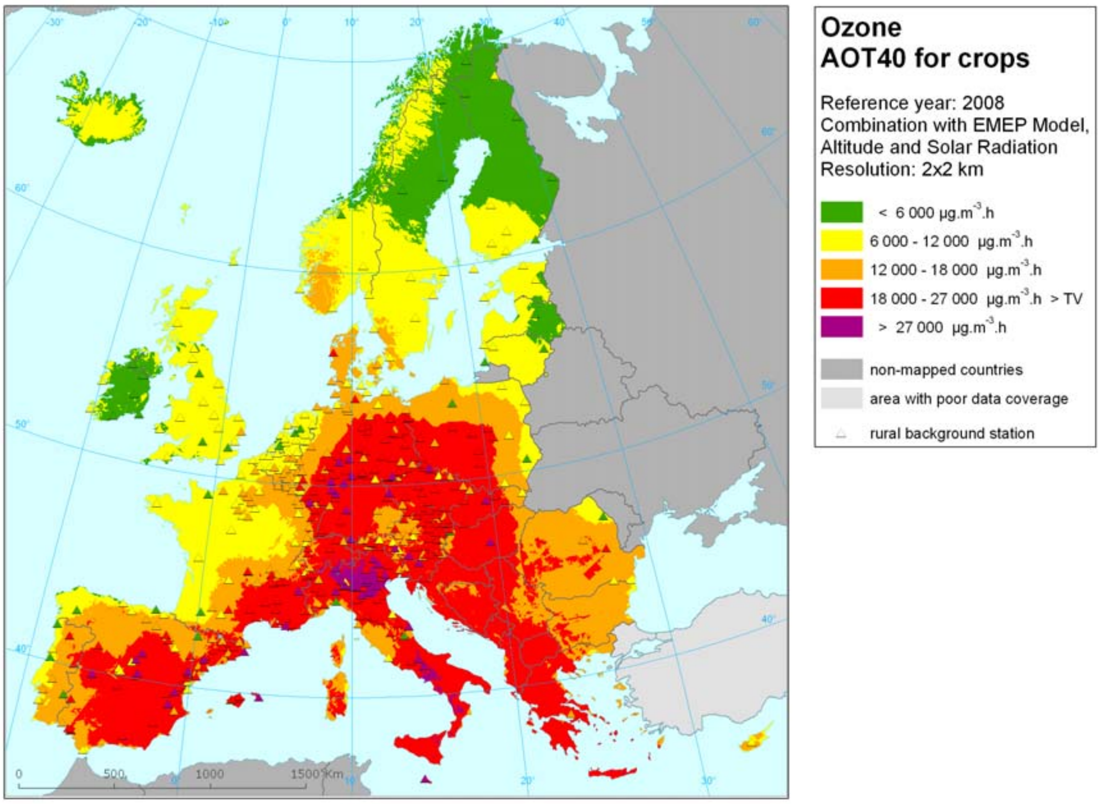

Figure 5.6 Rural concentration map of ozone vegetation indicator AOT40 for crops for the year 2007. Units: μg.m^{-3}.hours. Resolution: 2x2km^2.

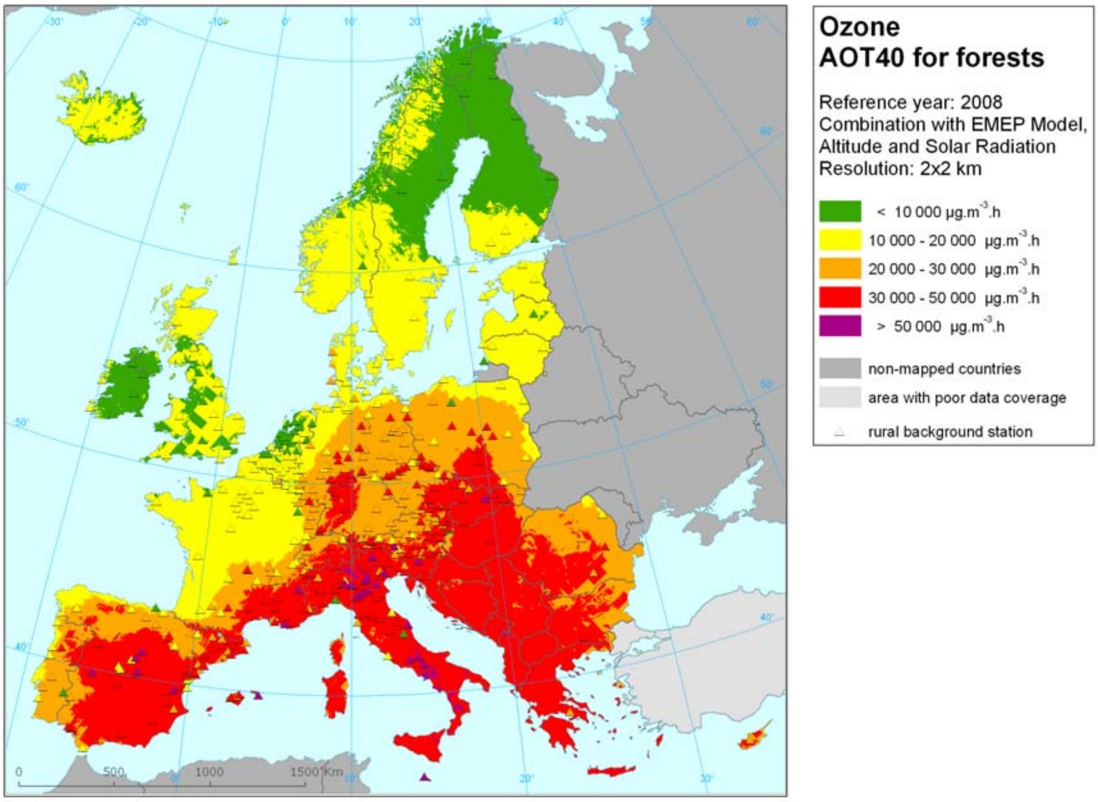

Figure 5.7 Rural concentration map of ozone vegetation indicator AOT40 for forests for the year 2008. Units: µg.m^{-3}.hours. Resolution: 2x2 km^2.

Both maps show for 2008, in continuation of 2007, a further decrease of the highest AOT40 levels (purple) throughout Europe. Only in Italy (Po Valley and the region around Naples), values in the highest class interval are still observed. On the other hand there is for AOT40 for forests in northern and north-west Europe a shift from the lowest two class intervals (green, yellow, orange; all below 20 mg.m-3.hours), to neighbouring higher class intervals. It concerns rather extended areas in a somewhat concentric-wise shape. For crops the same tendency is observed, where the extension of the orange areas means an exceedance of the Target Value. In addition, the 2008 map for crops shows also an extension of red areas that were in 2007 orange and neighbouring the red. This occurs on a rather large scale in Spain, France, Germany and Poland. The same happens with yellow neighbouring the orange in 2007 'turning' orange in 2008, for the same concentric zoning throughout Europe around the Po Valley as 'a kernel' for Europe.

5.3.2 Vegetation exposure

Agricultural crops

The rural map with ozone indicator AOT40 for vegetation, i.e. agricultural crops, as given in Figure 5.6 has been combined with the land cover CLC2000 map. Following a similar procedure as described in Horálek et al. (2007) the exposure of agricultural areas, defined as the Corine Land Cover level-1 class *2 Agricultural areas* (encompassing the level-2 classes *2.1 Arable land, 2.2 Permanent crops, 2.3 Pastures* and *2.4 Heterogeneous agricultural areas)* has been calculated at the country-level.

Table 5.8 gives the absolute and relative agricultural area for each country and for four European regions where the target value (TV) and long-term objective (LTO) for ozone are exceeded. The frequency distribution of the agricultural area per country over the exposure classes is presented as well.

Table 5.8 Agricultural area exposure and exceedance (Long Term Objective, LTO, and Target Value, TV) for ozone, AOT40 for crops, year 2008.

Country	Agricultural Area, 2008					Percentage of agricultural area, 2008 [%]				
	tot. area	> LTO (6 $mg.m^{-3}.h$)		> TV (18 $mg.m^{-3}.h$)		< 6	6 - 12	12 - 18	18 - 27	> 27
	[km^2]	[km^2]	[%]	[km^2]	[%]	$mg.m^{-3}.h$	$mg.m^{-3}.h$	$mg.m^{-3}.h$	$mg.m^{-3}.h$	$mg.m^{-3}.h$
Albania	7178	7178	100	6266	87.3	0	0	12.7	87.3	0.0
Austria	27502	27502	100	18504	67.3	0	0	32.7	67.3	0
Belgium	17648	17648	100	0	0	0	61.2	38.8	0	0
Bosnia-Herzegovina	19342	19342	100	15472	80.0	0	0	20.0	80.0	0.0
Bulgaria	57412	57412	100	1402	2.4	0	2.7	94.9	2.4	0
Croatia	24097	24097	100	23083	95.8	0	0	4.2	95.8	0
Cyprus	4297	4297	100	0	0	0	52.3	47.7	0	0
Czech Republic	45550	45550	100	45085	99.0	0	0	1.0	99.0	0
Denmark	32005	32005	100.0	0	0	0	14.5	85.5	0	0
Estonia	14654	13691	93.4	0	0	6.6	93.4	0	0	0
Finland	28822	16392	56.9	0	0	43.1	56.9	0	0	0
France (*)	328377	328362	100.0	33446	10.2	0.0	62.0	27.8	10.2	0.0
Germany	213406	213406	100.0	132081	61.9	0	3.2	34.9	61.8	0.1
Greece	51219	51219	100	40463	79.0	0	1.2	19.8	79.0	0.0
Hungary	63083	63083	100	52222	82.8	0	0	17.2	82.8	0
Iceland	2348	315	13	0	0	86.6	13.4	0	0	0
Ireland	46246	2663	6	0	0	94.2	5.8	0	0	0
Italy	155375	155375	100	130206	83.8	0	0.3	15.9	72.6	11.2
Latvia	28203	15129	53.6	0	0	46.4	53.6	0	0	0
Liechtenstein	43	43	100	43.5	100	0	0	0	100	0
Lithuania	40067	38543	96.2	0	0	3.8	96.2	0	0	0
Luxembourg	1427	1427	100	0	0	0	0	100	0	0
Macedonia, FYR	9509	9509	100	9494	99.8	0	0	0.2	99.8	0
Malta	122	122	100	122	100	0	0	0	100	0
Monaco	0.48	0.48	100	0.00	0	0	0	100	0	0
Montenegro	2400	2400	100	2262	94.2	0	0	5.8	94.2	0
Netherlands	24763	23708	95.7	0	0	4.3	93.9	1.8	0	0
Norway	15608	11226	71.9	0	0	28.1	67.6	4.3	0	0
Poland	200437	200437	100	77894	38.9	0	17.8	43.4	38.9	0
Portugal	42523	42523	100.0	866	2.0	0	22.1	75.9	2.0	0
Romania	134869	134869	100	13289	9.9	0	9.1	81.1	9.9	0
San Marino	46	46	100	46	100	0	0	0	100	0
Serbia (incl. Kosovo)	48529	48529	100	32726	67.4	0	0	32.6	67.4	0
Slovakia	24277	24277	100	19100	78.7	0	0	21.3	78.7	0
Slovenia	7114	7114	100	6803	95.6	0	0	4.4	95.6	0
Spain	252190	251292	99.6	147601	58.5	0.4	5.2	35.9	58.5	0.0
Sweden	38496	34468	89.5	0	0	10.5	76.2	13.3	0	0
Switzerland	11836	11836	100.0	7971	67.4	0	0	32.6	67.1	0.2
United Kingdom	141612	128861	91.0	0	0	9.0	91.0	0	0	0
Total	**2162634**	**2065897**	**95.5**	**816448**	**37.8**	**4.5**	**26.8**	**31.0**	**36.9**	**0.8**
(*) France N of 45N	260636	260621	100.0	9895	3.8	0.0	70.1	26.1	3.8	0
(*) France S of 45N	67741	67741	100	23551	34.8	0	30.6	34.6	34.8	0.0
Northern	197855	161455	81.6	0	0					
North-western	494681	435243	88.0	9895	2.0					
Central & eastern	778416	778416	100	367593	47.2					
Southern	691682	690784	99.9	438960	63.5					
Total	**2162634**	**2065897**	**95.5**	**816448**	**37.8**					

Note: Countries not included due to lack of land cover data: Andorra, Turkey.

The table indicates the country grouping with corresponding colours of the region; *Northern Europe*: Sweden, Finland, Norway, Estonia, Lithuania, Latvia and Denmark. *North-western Europe*: United Kingdom, Ireland, Iceland, the Netherlands, Belgium, Luxembourg and France north of 45 degrees latitude. *Central and Eastern Europe*: Germany, Poland, Czech Republic, Slovakia, Hungary, Austria, Liechtenstein, Bulgaria and Romania. *Southern Europe*: Albania, Bosnia-Herzegovina, France south of 45 degrees latitude, Portugal, Spain, Italy, San Marino, Slovenia, Croatia, Greece, Cyprus, F.Y.R. of Macedonia, Montenegro, Serbia and Malta.

Table 5.8 illustrates that in 2008 about 38 % of all European agricultural land was exposed to ozone exceeding the target value (TV) of 18 $mg.m^{-3}.h$ and about 96 % was exposed to levels in excess of the long-term objective (LTO) of 6 $mg.m^{-3}.h$. This is a slight rise in the total area with agricultural crops above the TV and considered to suffer from adverse effects to ozone exposure compared to 2007 (36 %), but still well below 2006 (70 %) and 2005 (49 %). Considering the long-term objective the area in excess increased again to levels well above 2007 (78 %) and close to 2006 (98 %) and 2005 (89 %). Contrary to 2007, in 2008 not one European country had ozone levels not being in excess of the LTO. Only Finland and Iceland show a limited percentage of their crops exposed to levels above the LTO and for Finland and Latvia about half of their crops. For the remainder of the countries more than 90 % (often even 100 %) of the agricultural areas are submitted to AOT40 in excess of the LTO. In many countries of central and southern Europe more than half of their total agricultural area experienced exposures above the target value as least stringent threshold.

In southern Europe, about 64 % of the total agricultural area exceeds in 2008 the target value. In the same region about 55 % of the total agricultural area exceeds the target value in 2007. This is an increase of 9 % compared to 2007, but still substantially below the amounts of 2006 (94 %) and 2005 (96 %). In 2008, 2007 and 2005 no area is mapped in excess of the target value in northern Europe; only in 2006 about 4 % of its area was in excess of the target value. In the north-western region the area exceeding the target value is almost 50 % in 2006, which is more than four times larger than in 2005 (11 %). However, in 2007 ozone levels have dropped such that only less than 1 % of the area is still in excess and in 2008 about 2 %. For the central and eastern region, the total area where ozone exceeds the target value increased considerably from 2005 to 2006: from 44 % to 77 %. In 2007 it drops to an area of 50 % and in 2008 it is further reduced to 47 % of the total area, being just above the level of 2005. Compared to 2005, the frequency distribution of agricultural area over the exposure classes shows for 2006 a clear shift towards higher exposures leading to an increased total area exceeded. In 2007, this shift diminishes again to a distribution more similar to that of 2005, with even a small increase in the area not exceeding the target value. In 2008, this tendency continues with about a similar area percentage in excess of the TV, however, including a shift of areas percentages with the lower exposure levels in 2007 to the somewhat higher levels in 2008, but still below the target value.

Forests

The rural map with ozone indicator AOT40 for forests, as given in Figure 5.7, has been combined with the land cover CLC2000 map as well. Following a similar procedure as described in Horálek et al. (2007) the exposure of forest areas, defined as the Corine Land Cover level-2 class *3.1. Forests,* has been calculated at the country-level.

Table 5.9 gives for each country, four European regions and Europe as a whole the absolute and relative forest area where – let us call it – the *Reporting Value* (RV of 20 $mg.m^{-3}.h$, as Annex III of the ozone directive defines it) in combination with the *Critical Level* (*CL* of 10 $mg.m^{-3}.h$, as defined in the Mapping Manual) are exceeded. The table presents the frequency distribution of the forest area per country over the exposure classes as well. The Reporting Value of the ozone directive (RV) of 20 $mg.m^{-3}.h$ is exceeded in 2008 at 50 % of the total European forest area, which is about the same as in 2007, while in 2006 it was almost 70 % and in 2005 about 60 %. This means that the area of forest exposed to levels above the accumulated ozone Reporting Value initially increased in 2006 with 10 % and than diminished again in 2007 and 2008 to a smaller area of even 10 % below that of 2005. In 2005 three-quarters of the European forest area exceeded the Critical Level of 10 $mg.m^{-3}.h$. In 2006 in about all forested areas the Critical Level was exceeded. This reduced again in 2007 to almost two-third of the total, but in 2008 it increased to 80 %. All European countries had forests exposed to accumulated ozone concentrations above the Critical Level, while for most even all their forests suffered exposure to levels in excess of the least stringent Reporting Value. Parallel to the agricultural thresholds, Finland, Sweden, Norway, Iceland, Ireland, The Netherlands and the UK showed in 2007 accumulated ozone levels not exceeding the reporting level and only for a part of their forests exceeding the Critical Level. Estonia and Latvia showed only a few percent of their forest area not exposed to levels exceeding the Critical Level as most stringent.

As in previous years, in 2008 the southern European region had AOT40 levels where about all forested areas exceed the Critical Level. The central and eastern regions show over the four years a continued 100 % exceedance of the Critical Levels, whereas the area exceeding the Reporting Value shows a peak of 100 % in 2006 followed by a reduction to about 85 % in 2007, but followed by an increase of about 15 % in 2008 to 94 %, and coming close to the 96 % of 2005. In the north-western region the area exceeding the Critical Level increases from 84 % in 2005 to practically the whole area (98 %) in 2006. In 2007 it dropped again to 78 % but in 2008 it increased to almost all forested area (94 %). Concerning the forested area above the Reporting Value there was an increase observed from 69 % in 2005 to 80 % in 2006, with a prominent drop in 2007 to 28% that continued in 2008 to 24 %. Specifically in the northern region of Europe, the area in exceedance peaks considerably in 2006: the area above the Critical Level enlarges from 40 % in 2005 to even 100 % in 2006 and reduces thereafter to just 12 % in 2007 and increased in 2008 to 51 %. The Reporting Value peaks from no exceedance in 2005 to 23 % in 2006 back to none in 2007 and 2008. In comparison with 2005, the frequency distribution of the forested area over the exposure classes for 2006 shows a clear shift to higher exposures, specifically for the areas which had the lowest class values and values well above the Reporting Value in 2005. In 2007 an opposite shift occurs back to the lower neighbouring classes and for a more extended area than in 2005. In 2008 a shift was observed of areas exposed in 2007 to the highest exposures to its neighbouring lower class interval and for the areas exposed in 2007 to the lowest exposure class to its neighbouring higher class interval. The total area with AOT40 levels below the Critical Level diminished by 18 % in 2008 (20 %) compared to 2007 (38.5 %); the total area submitted to levels below the Reporting Value was with about 50 % the same in both years.

Table 5.9 Forest area exposure and exceedance (Critical Level, CL, and Reporting Value, RV) for ozone, AOT40 for forests, year 2008.

Country	Area of forests, 2008					Percentage of forest area, 2008 [%]				
	tot. area	> CL (10 $mg.m^{-3}.h$)		> RV (20 $mg.m^{-3}.h$)		< 10	10 - 20	20 - 30	30 - 50	> 50
	[km^2]	[km^2]	[%]	[km^2]	[%]	$mg.m^{-3}.h$	$mg.m^{-3}.h$	$mg.m^{-3}.h$	$mg.m^{-3}.h$	$mg.m^{-3}.h$
Albania	7818	7818	100	7818	100	0	0	0	97.4	2.6
Austria	37613	37613	100	37613	100	0	0	47.3	52.7	0
Belgium	6090	6029	99.0	0	0	1.0	99.0	0	0	0
Bosnia-Herzegovina	22952	22952	100	22952	100	0	0	0.8	99.1	0.0
Bulgaria	34821	34821	100	34821	100	0	0	19.6	80.4	0
Croatia	20140	20140	100	20140	100	0	0	1.2	98.8	0
Cyprus	1551	1551	100	1551	100	0	0	26.5	73.5	0
Czech Republic	25455	25455	100	25455	100	0	0	57.6	42.4	0
Denmark	3641	3641	100	61	1.7	0	98.3	1.7	0	0
Estonia	20767	20687	99.6	0	0	0.4	99.6	0	0	0
Finland	193292	46061	23.8	0	0	76.2	23.8	0	0	0
France (*)	144835	144788	100.0	69552	48.0	0.0	51.9	25.8	22.2	0
Germany	103822	103822	100	96304	92.8	0	7.2	76.9	15.8	0
Greece	23538	23538	100	23538	100	0	0	3.6	95.9	0.5
Hungary	17341	17341	100	17341	100	0	0	11.3	88.7	0
Iceland	314	147	47	0	0	53.1	46.9	0	0	0
Ireland	2906	252	8.7	0	0	91.3	8.7	0	0	0
Italy	78783	78783	100	78783	100	0	0	1.4	89.8	8.8
Latvia	26915	26167	97.2	0	0	2.8	97.2	0	0	0
Liechtenstein	67	67	100	67	100	0	0	41.6	58.4	0
Lithuania	18659	18659	100	0	0	0	100	0	0	0
Luxembourg	908	908	100	67	7.4	0	92.6	7.4	0	0
Macedonia, FYR	8641	8641	100	8641	100	0	0	0	99.8	0.2
Malta	2	2	100	2	100	0	0	0	100	0
Monaco	1	1	100	1	100	0	0	0	100	0
Montenegro	5776	5776	100	5776	100	0	0	0	98.6	1.4
Netherlands	3101	2118	68.3	0	0	31.7	68.3	0	0	0
Norway	104751	68650	65.5	3	0.0	34.5	65.5	0.0	0	0
Poland	91804	91804	100	74977	81.7	0	18.3	67.9	13.7	0
Portugal	24299	24299	100	21652	89.1	0	10.9	83.2	5.9	0
Romania	69775	69775	100	69530	99.6	0	0.4	44.0	55.6	0
San Marino	7	7	100	7	100	0	0	0	100	0
Serbia (incl. Kosovo)	26707	26707	100	26707	100	0	0	0.9	99.1	0.1
Slovakia	19322	19322	100	19322	100	0	0	13.5	86.5	0
Slovenia	11486	11486	100	11486	100	0	0	2.1	97.9	0
Spain	91844	91844	100	82480	89.8	0	10.2	27.7	62.2	0
Sweden	249830	128679	51.5	0	0	48.5	51.5	0	0	0
Switzerland	12531	12531	100	12531	100	0	0	53.4	46.0	0.6
United Kingdom	19617	15860	80.8	0	0	19.2	80.8	0.0	0	0
Total	**1531721**	**1218740**	**79.6**	**769174**	**50.2**	**20.4**	**29.4**	**20.2**	**29.5**	**0.5**
(*) France N of 45N	89510	89462	99.9	28451	31.8	0.1	68.2	28.2	3.6	0
(*) France S of 45N	55326	55326	100.0	41101	74.3	0	25.7	22.0	52.3	0
Northern	617854	312544	50.6	64	0.0					
North-western	122447	114777	93.7	28518	23.3					
Central & eastern	412551	412551	100	387959	94.0					
Southern	378869	378869	100	352633	93.1					
Total	**1531721**	**1218740**	**79.6**	**769174**	**50.2**					

Note: Countries not included due to lack of land cover data: Andorra, Turkey.

5.3.3 Uncertainties

Uncertainty estimated by cross-validation

In Table 5.7 the absolute mean uncertainty (RMSE) obtained by cross-validation is 5283 $\mu g.m^{-3}.h$ for the AOT40 for crops and 8750 $\mu g.m^{-3}.h$ for the AOT40 for forests. It indicates that the year 2008 has lower absolute mean uncertainties for the crops and forests than 2007 (5876 and 10190 $\mu g.m^{-3}.h$), 2006 (7674 and 11990 $\mu g.m^{-3}.h$) and 2005 (7700 and 12500 $\mu g.m^{-3}.h$).

The relative mean uncertainty of the 2008 map of ozone indicator AOT40 for crops is about 31% and of the map of AOT40 for forests about 34 %. These relative uncertainties are of the same level as for the 2006 maps (30 and 34 %) and lower than those of the maps of 2007 (40 and 37 %) and 2005 (41 and 42 %).

Figure 5.9 shows the cross-validation scatter plots of the AOT40 for both crops and forests. R^2 indicates that for AOT40 for crops about 53 % and for AOT40 for forests about 56 % of the variability is attributable to the interpolation. The corresponding values for the 2007 maps (63 % and 67 %), the 2006 maps (47 % and 49 %) and 2005 maps (55 % and 58 %), indicates a somewhat reduced level of interpolation performance at the 2008 maps compared to those of 2007 and 2005, but being more on the same for crops and better for forests than for those of 2006.

The cross-validation scatter plots show again that in areas with higher accumulated ozone concentrations the interpolation methods tend to deliver seriously underestimated predicted values. For example, in agricultural areas (Figure 5.9, left panel) an observed value of 30 000 $\mu g.m^{-3}.h$ is estimated in the interpolation as about 24 000 $\mu g.m^{-3}.h$, i.e. an underestimation of about 20 %. In addition, an overestimation at the lower end of predicted values occurred. One could reduce this under- and overestimation by extending the number of measurement stations and by optimising the spatial distribution of those stations, specifically in areas with elevated values.

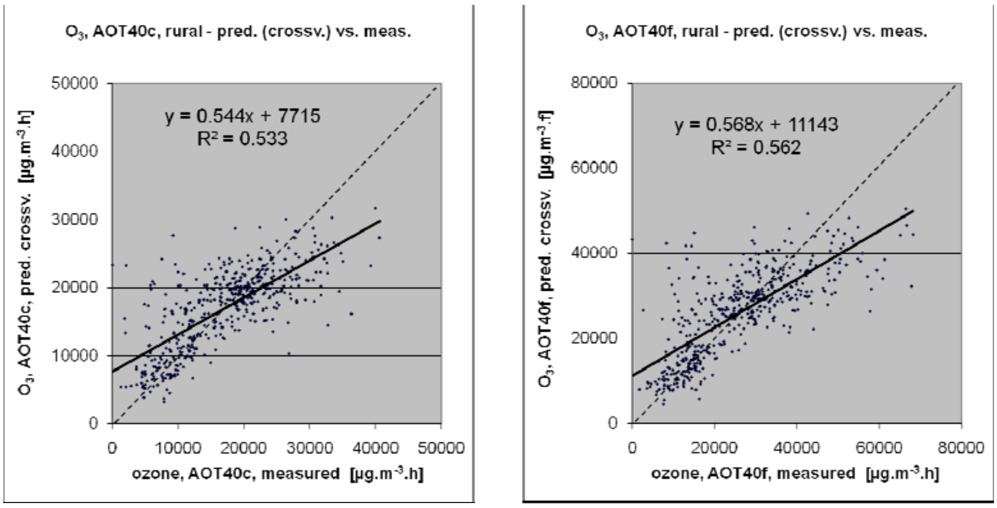

Figure 5.9 Correlation between cross-validation predicted values (y-axis) and measurements (x-axis) for the ozone indicators AOT40 for crops (left) and AOT40 for forests (right) for rural areas in 2008.

Comparison of point measurement values with the predicted grid value

Additional to the point observation - point prediction cross-validation, a simple comparison has been made between the point measurement and interpolated predicted grid values averaged in a 2 x 2 km^2 grid. The results of the cross-validation compared to the gridded validation are summarised in Table 5.10. The table shows for both receptors a better correlation between the station measurements and the averaged interpolated predicted values of the corresponding grid cells (case ii) than it does at the point cross-validation predictions (case i) of Figure 5.9. Case ii) represents the uncertainty in the predicted gridded interpolation map at the actual station locations (points) itself, whereas the point observation –

point prediction cross-validation of case i) simulates the behaviour of the interpolation at point positions without actual measurements within the area covered by measurements. The uncertainty at measurement locations is caused partly by the smoothing effect of interpolation and partly by the spatial averaging of the values in the 2 x 2 km^2 grid cells. The level of the smoothing effect leading to underestimation at areas with high values is there smaller than it is in case no measurement is present in such areas. For example, in agricultural areas the predicted interpolation grid value will be about 25 500 $\mu g.m^{-3}.h$ at the corresponding station point with the observed value of 30 000 $\mu g.m^{-3}.h$, i.e. an underestimation of about 15 %.

Table 5.10 Linear regression equation and coefficient of determination R^2 from the scatter plots of (i) the predicted point values based on cross-validation and (ii) aggregation into 2x2 km^2 grid cells versus the measured point values for PM_{10} indicator annual average for rural (left) and urban (right) areas of 2008.

	AOT40 for crops		**AOT40 for forests**	
	equation	R^2	**equation**	R^2
i) cross-validation prediction (Fig 5.9)	y = 0.544x + 7715	0.533	y = 0.568x + 11143	0.562
ii) 2x2 km grid prediction	y = 0.655x + 5825	0.740	y = 0.644x + 9184	0.711

The AOT40 for crops with a target value of 18 000 $\mu g.m^{-3}.h$ would allow us to prepare a probability of exceedance map. However, we limited the preparation of such maps to the human health related indicators, thus not involving the accumulative ozone indicators used in the EEA CSI005, not demanding such maps.

6 Concluding exposure and uncertainty estimates

Mapping and exposure results

This paper presents the interpolated maps for 2008 on the PM_{10} and ozone human health related air pollution indicators, together with their frequency distribution of the estimated population exposures and exceedances. It concerns the annual average and the 36^{th} maximum daily mean for PM_{10} and the SOMO35 for ozone. Additionally, presented are for ozone the interpolated maps on the ecosystem based indicators AOT40 for crops and AOT40 for forests, including their frequency distribution of estimated land area exposures and exceedances. A similar mapping approach, primarily based on station observational data, has been used as in previous years (De Smet et al. (2010) and references cited therein).

Human health PM_{10} indicators

Table 6.1 summarises for both *human health PM_{10} indicators* the average concentration the European inhabitant is exposed to, i.e. the population-weighted concentration, and the number of Europeans exposed to PM_{10} concentrations above their limit values (LV) for the years 2005 to 2008. The table presents the results obtained with the merging resolution on both the 10x10 km^2 grid as used at previous data years, and the 1x1 km^2 grid as tested with the 2006 data in Horálek et al (2010) and implemented fully for the 2008 data. It provides an indication that the underestimation of PM10 values at merging with the 10x10 km^2 grid resolution has been resolved better when using a higher 1x1 km^2 grid resolution. In other words, an increased merging resolution contributes to a quantitatively better population exposure estimate due to better resolving the spatially smaller urbanised patterns in the map.

Table 6.1 Percentage of the total European population exposed to PM_{10} concentrations above the limit values (LV) and the population-weighted concentration for the human health PM_{10} indicators annual average and 36th maximum daily average for 2005 to 2008.

PM10			2005	2006	2007	2008
Annual average						
Population-weighted concentration	(µg.m^{-3})	10x10 merger	26.3	27.1	25.3	
		1x1 merger		28.5		24.8
Population exposed > LV (40 µg.m^{-3})	(% of total)	10x10 merger	9.3	7.7	5.7	
		1x1 merger		9.8		5.8
36th max. daily average						
Population-weighted concentration	(µg.m^{-3})	10x10 merger	43.8	45.4	42.4	
		1x1 merger		47.8		41.3
Population exposed > LV (50 µg.m^{-3})	(% of total)	10x10 merger	28.1	28.5	22.0	
		1x1 merger		35.7		19.4

The population exposed to *annual mean* concentrations of PM_{10} above the limit value of 40 µg.m^{-3} is at least 6 % of the total population in 2008. Furthermore, it is estimated that the European inhabitants living in the background (neither hot-spot nor industrial) areas – without regard to urban or rural – are exposed on average to the annual mean PM_{10} concentration of 25 µg.m^{-3}. In comparison with the previous three years, the number of people living in the areas above the LV originally tends to go down slightly. This trend is unlikely to be significant when taking into account the increased merging resolution applied on the 2008 data and the meteorologically induced variations and the uncertainties involved in the interpolation. Longer time series and reduced uncertainties will be needed before drawing any conclusions on a possible trend.

In 2008 at least 19 % of the European population lived in areas where the PM_{10} limit value of 50 µg.m^{-3} for the *36^{th} maximum daily mean* is exceeded, being some 2-3 % lower than in 2007 and 8-9 % lower than in 2006 and 2005. The overall European population-weighted concentration of the 36th maximum daily mean for the background areas is estimated at about 41 µg.m^{-3}. Compared to the previous three years one cannot simply conclude on some tendency, except that in 2008 and 2007 the highest daily averages had lower concentrations than in 2006 and 2005, probably leading to a population exposed to slightly lower concentrations. Mind that the increased merging resolution applied on the 2008 data leads to reduced underestimations. That in itself leads to an increased number of the population exposure and subsequently strengthens the confirmation of the lower concentration exposures in 2008.

Comparing the observed exceedances for both PM_{10} indicators, one can conclude that the daily limit value is the most stringent throughout the years.

Human health ozone indicators

Table 6.2 summarises for both *human health ozone indicators* the average concentration the European inhabitants are exposed to, i.e. the population-weighted concentration. Furthermore, the number of Europeans exposed to concentrations above the limit values of the 26th highest daily maximum 8-hour mean and above a level of 6 mg.m^{-3}.d for the SOMO35 for the years 2005 to 2008 is presented. The table presents the results obtained with the merging resolution on both the 10x10 km^2 grid as used at previous data years, and the 1x1 km^2 grid as tested on the 2006 data in Horálek et al (2010) and implemented fully for the 2008 data. It provides an indication that the overestimation of ozone values at merging with the 10x10 km^2 grid resolution has been resolved better when using a higher 1x1 km^2 grid resolution. In other words, an increased merging resolution contributes to a quantitatively better population exposure estimate due to better resolving the spatially smaller urbanised patterns in the map.

Table 6.2 Percentage of the total European population exposed to ozone concentrations above the target value (TV) for the 26th highest daily maximum 8-hour average and an indicative chosen threshold for SOMO35, including their population-weighted concentrations for2005 to 2008.

Ozone			2005	2006	2007	2008
26th highest daily max. 8-hr average						
Population-weighted concentration	(µg.m^{-3})	10x10 merger	112.9	119.6	112.1	
		1x1 merger		118.2		109.8
Population exposed > TV (120 mg.m^{-3}.h)	(% of total)	10x10 merger	37.8	55.5	33.5	
		1x1 merger		51.4		15.0
SOMO35						
Population-weighted concentration	(µg.m^{-3})	10x10 merger	5047	5485	4679	
		1x1 merger		5167		4275
Population exposed > 6 mg.m^{-3}.d	(% of total)	10x10 merger	33.9	37.4	32.6	
		1x1 merger		29.5		19.6

For the ozone indicator *26th highest daily maximum 8-hour mean* it is estimated that at least 15 % of the population lived in 2008 in areas above the ozone target value (TV) of 120 µg.m^{-3}. The overall European population-weighted ozone concentration in terms of the 26th highest daily maximum 8-hour mean in the background areas is estimated at almost 110 µg.m^{-3}. Compared to the previous three years one could conclude that 2006 is a year with elevated ozone concentrations, leading to increased exposure levels compared to 2005, 2007 and 2008. Additionally, in 2008 the population exposed to ozone level above the target value is substantially lower than in the previous three years. The increased merging resolution will have partially caused the reduced value.

Similar tendency is observed for the *SOMO35*: in 2005 and 2007 one-third of the population lived in areas where a level of 6 mg.m^{-3}.d(*) was exceeded and being slightly lower than the estimated 37 % in 2006. In 2008 it concerns only one-fifth of the population. The population weighted SOMO35 concentrations shows a similar pattern. The increase of 2006 occurs specifically in areas of northern and north-western Europe where the lowest SOMO35 levels are found. In 2008 however, these reduced levels did show up less prominently. Some limited reductions in 2007 and 2008 are found on the Iberian Peninsula.

(*) Note that the 6 mg.m^{-3}.d does not represent a legally binding 'threshold'. In this and previous papers it concerns a somewhat arbitrarily chosen threshold to be able to discuss the observed distributions of SOMO35 levels in their spatial and temporal context. This choice is based on a comparison of the 26th highest daily max. 8-hour means versus the SOMO35 of the ozone concentration measurements at all background stations in The Netherlands. The SOMO35 is estimated to be about 4 mg.m^{-3}.d when no Dutch population is exposed to ozone concentrations above the target value of the 26th h.d.m.8-hour mean. The Netherlands has in general relative low ozone concentrations compared to most other European countries. Over the years we applied the level of 6 mg.m^{-3}.d in our discussions of the annual results for two reasons: (i) to compensate for a possible underestimation of the SOMO35, and (ii) to match with a class interval limit of the SOMO35 map (Figure 5.4).

Agricultural and forest ozone indicators

Exposure indicators describing the *agricultural and forest areas exposed to accumulated ozone* concentrations above defined thresholds are summarised in Table 6.3. They are the target value (LV) of 18 mg.m^{-3}.h and the long-term objective (LTO) of 6 mg.m^{-3}.h for the AOT40 for crops, and the Reporting Value (RV) of 20 mg.m^{-3}.h and the Critical Level (CL) of 10 mg.m^{-3}.h for the AOT40 for forests.

Table 6.3 Percentages of the total European agricultural and forest area exposed to ozone concentrations above their thresholds: target value (TV) and long-term objective (LTO) for AOT40 for crops, and Critical Level (CL) and Reporting Value (RV) for AOT40 for forests for2005 to 2008.

Ozone		2005	2006	2007	2008
AOT40 for crops					
Agricultural area % > TV (18 mg.m^{-3}.h)	(% of total)	49	70	36	38
Agricultural area % > LTO (6 mg.m^{-3}.h)	(% of total)	89	98	78	96
AOT40 for forests					
Forest area exposed > RV (20 mg.m^{-3}.h)	(% of total)	59	69	48	50
Forest area exposed > CL (10 mg.m^{-3}.h)	(% of total)	76	100	62	80

In 2008, about 38 % of all agricultural land is exposed to accumulated ozone concentrations exceeding the target value and about 96 % is exposed to levels in excess of the long-term objective. Compared to the previous three years one could conclude that 2006 is a year with elevated ozone concentrations leading to increased exposure levels above the target value (TV) and that they subsided in 2007 and 2008 to levels clearly below those of 2005. On the other hand, the percentage of the total area exposed to levels above the long-term objective (LTO) is in 2007 lowest compared to the years 2005, 2006 and 2008.

For the ozone indicator AOT40 for forests the level of 20 mg.m^{-3}.h is in 2008 was exceeded in about 50 % of the European forest area, which is similar to 2007 and clearly below the percentages of the years 2005 and 2006. A rather similar development is observed for the forest area exceeding the Critical Level, however with a somewhat more elevated Critical Level exceedance in 2008 than in 2007.

The temporal pattern of the AOT40 for forests exceedances shows large similarity with those of the AOT40 for crops despite their different definitions. The annual variability has its cause in its known strong correlation to and dependency on the meteorological variability.

The results in this report show that in general over Europe, and most significantly over northern and north-western Europe, 2006 was characterised by higher ozone levels than in 2005, 2007 and 2008: all indicators show an increase in 2006. It furthermore shows that 2008 was characterised by having less areas with concentration levels at the lower end, below the LTO and CL, than in 2005 and 2007.

Uncertainty results

Next to the creation of European wide interpolated air pollutant maps and exposure tables, the uncertainty of the presented maps has been evaluated and maps with estimated probability of threshold exceedance have been derived for the human health indicators. As exactly the same method and data sources has been applied over the years 2005 to 2008 a change in uncertainty is in principle related to the data content itself, meaning not within our span of control. This is however, not completely true. For the 2008 data year we implemented for the first time an increased resolution (from a 10x10 km^2 into 1x1 km^2 grid field) at the merging of the separate human health indicator interpolated maps (on 10x10 km^2 grid) into one combined final 1x1 km^2 gridded indicator map. The merging made use of the 1x1 km^2 population density map. Exposure estimates have been based on the 10x10 km^2 grid fields as result of the aggregation of the 1x1 km^2 grids. This increased merging resolution should in principle improve the accuracy in the concentration maps, and reduce the interpolation uncertainty of these maps, including the subsequent exposure estimates. Denby et al. (2009) discusses a diversity of uncertainty factors potentially involved, including their possible levels of influence. The paper recommends options to reduce uncertainties systematically. Horálek et al. (2010) explored specific options to reduce interpolation uncertainty related to the spatial resolutions applied at the different process steps of the mapping method. This paper concludes and justifies the implementation of the increased merging grid as most significant uncertainty reduction measure, against the least additional demands.

Table 6.4 summarises the absolute and relative mean interpolation uncertainties of the PM_{10} maps for the four years sequence. The uncertainties in 2007 are slightly lower than in 2008, 2006 and 2005; this is probably given by the better fit of the linear regression with supplementary data in 2007 compared to the three other years.

Table 6.4 Absolute mean uncertainty (RMSE, $\mu g.m^{-3}$) and relative mean uncertainty (RMSE relative to mean indicator value, in %) for the total European rural and urban areas for PM_{10} annual average and the 36th maximum daily average for the years 2005 – 2008.

PM10			2005	2006	2007	2008
Annual average						
rural areas	abs. mean uncertainty	RMSE ($\mu g.m^{-3}$)	5.5	5.8	4.6	5.0
	rel. mean uncertianty	%	*25*	*27*	*24*	*27*
urban areas	abs. mean uncertainty	RMSE ($\mu g.m^{-3}$)	5.5	6.1	5.0	6.3
	rel. mean uncertianty	%	*20*	*21*	*18*	*22*
36th max. daily average						
rural areas	abs. mean uncertainty	RMSE ($\mu g.m^{-3}$)	9.8	13.3	8	8.8
	rel. mean uncertianty	%	*27*	*26*	*24*	*28*
urban areas	abs. mean uncertainty	RMSE ($\mu g.m^{-3}$)	11.7	9.9	9.1	12.7
	rel. mean uncertianty	%	*24*	*21*	*20*	*24*

The relative mean interpolation uncertainty of the ozone maps in Table 6.5 were similar in 2008 and 2007 and only for the AOT40 indicators these values are clearly different (lower) than those of the years 2005 and 2006. In general, a continuous decrease in the absolute mean uncertainties can be observed throughout the four years, with the clearest effect for the AOT40.

Table 6.5 Absolute and relative mean uncertainty for the total European areas for ozone the 26th highest daily maximum 8-hour average, SOMO35, AOT40 for crops and for forests, for the years 2005 – 2008.

Ozone			2005	2006	2007	2008
26th highest daily max. 8-hr average						
rural areas	abs. mean uncertainty	RMSE (μg.m^{-3})	12.3	11.2	8.8	8.7
	rel. mean uncertianty	%	*10*	*9*	*8*	*8*
urban areas	abs. mean uncertainty	RMSE (μg.m^{-3})	10.0	10.2	8.9	8.8
	rel. mean uncertianty	%	*9*	*8*	*8*	*8*
SOMO35						
rural areas	abs. mean uncertainty	RMSE (μg.m^{-3}.d)	2173	2077	1801	1609
	rel. mean uncertianty	%	*36*	*32*	*33*	*31*
urban areas	abs. mean uncertainty	RMSE (μg.m^{-3}.d)	1459	1472	1260	1293
	rel. mean uncertianty	%	*32*	*29*	*30*	*31*
AOT40 for crops						
rural areas	abs. mean uncertainty	RMSE (μg.m^{-3}.h)	7700	7674	5876	5283
	rel. mean uncertianty	%	*41*	*40*	*30*	*31*
AOT40 for forests						
rural areas	abs. mean uncertainty	RMSE (μg.m^{-3}.h)	12500	11990	10190	8750
	rel. mean uncertianty	%	*42*	*37*	*34*	*34*

The scatter plots of the interpolation results versus the measurements show that for both the PM_{10} and the ozone indicators in areas with high values, a systematic underestimation of the predicted values occurs, leading also to a considerable underestimation at locations without measurements. This effect is demonstrated most prominently by the ozone indicators. It is expected that the underestimation will be reduced when an improved fit of the linear regression with (other) supplementary data could be reached. For example, in the near future more contributions from satellite imagery data and interpretation techniques are expected. Other options are extending the number of measurement stations and/or using additional mobile stations (e.g. in measurement campaigns). Continued efforts aiming for a more optimised spatial distribution of (such) stations, especially in areas with high air pollution, and reduction of external uncertainties would certainly contribute to reducing uncertainties in the interpolations. For further reading on this subject we refer to Denby et al. (2009) and forthcoming ETC/ACC Technical Papers.

Probability of exceedance

Maps with the probability of exceedance of Limit Values or Target Value have been prepared for the human health indicators of PM_{10} and ozone only. These probability maps, with a class distribution as defined in Table 4.4, are derived from combining the indicator map and its uncertainty map following the same method throughout the years 2005 to 2008. The differences in the maps between years depend on annual fluctuation in concentration levels, supplementary data and their involved uncertainties. Explaining their systematic relation is difficult, since their direct causes are still a matter of study (Denby et al. 2009). Some disruption or 'jump' could be expected between the data of 2005-2007 and 2008. This would then be caused by the increased merging resolution applied for the first time on the 2008 data. As Horálek et al. (2010) indicated, it should improve the interpolation accuracy and reduce the interpolation uncertainty, specifically for urban areas that profit most of this methodological refinement. However, the data in the tables of this paper do not show a clear effect that can be deduced from this fine-tuning of the mapping methodology. We assume in the first instance, however without proof, that this improvement is masked by the annual variability of the data inherent to the used data sources.

For the annual average PM_{10} the patterns in the spatial distribution of the different probability of exceedance (PoE) classes over Europe in 2008, in general, slightly reduced further compared to 2007, 2006 and 2005.

The 36th maximum daily means of PM_{10} do show in 2008, in general, throughout Europe, a further reduction of both the extent of areas and the elevation of its levels of likelihood of exceedances. In many areas, these reductions consist of shifts to one lower PoE class, except at some of the kernels of agglomerations and industrial regions where elevated PoE continue to exist. In these areas considerable systematic emission reductions may still be needed to reach non-exceedance levels in the future.

Interpreting 2008 with its previous years, one can conclude for ozone that in 2006 the probability of exceedance (PoE) for the ozone increased temporarily in most parts of Europe. In 2007 and 2008, Central Europe showed a continued and well-observed decrease of PoE to levels, in many areas well below those of 2005. Most areas with serious PoE in 2007 showed in 2008 moderate and even modest levels of PoE, except for the northern and more southern region of Italy, parts of Greece, inner Spain and the more south-western German region, where in 2008 unchanged likelihood of exceedances occurred. Forthcoming years may have to confirm whether this is a manifestation of a significant positive trend.

References

AirBase, European air quality database, http://airbase.eionet.europa.eu
Benedictow A et al (2010). Transboundary acidification, eutrophication and ground level ozone in Europe in 2008. EMEP Report 1/2010. http://emep.int/publ/reports/2010/status_report_1_2010.pdf
Cressie N (1993). Statistics for spatial data. Wiley series, New York.
De Leeuw F, Horálek J (2009). Assessment of the health impacts of exposure to PM2.5 at a European level. ETC/ACC Technical Paper 2009/1. http://air-climate.eionet.europa.eu/reports/ETCACC_TP_2009_1_European_PM2.5_HIA
De Leeuw F, Fiala J (2009). Indicators on Urban Air Quality - A review of current methodologies. ETC/ACC Technical Paper 2009/8. http://air-climate.eionet.europa.eu/reports/ETCACC_TP_2009_8_UrbanAQindicators
De Leeuw F, Horálek J, Denby B, de Smet P (2010). Assessment of the health impacts of exposure to PM2.5 at a European level. Atmospheric Environment. (Accepted, Nov 2010).
Denby B, Horálek J, Walker SE, Eben K, Fiala J (2005). Interpolation and assimilation methods for European scale air quality assessment and mapping. Part I: Review and recommendations. ETC/ACC Technical paper 2005/7. http://air-climate.eionet.europa.eu/docs/ETCACC_TechnPaper_2005_7_SpatAQ_Interpol_Part_I.pdf
Denby B, Schaap M, Segers A, Builtjes P, Horálek J (2008). Comparison of two data assimilation methods for assessing PM_{10} exceedances on the European scale. Atmospheric Environment 42, 7122–7134.
Denby B, De Leeuw F, De Smet P, Horálek J (2009). Sources of uncertainty and their assessment in spatial mapping, ETC/ACC Technical Paper 2008/20. http://air-climate.eionet.europa.eu/reports/ETCACC_TP_2008_20_spatialAQ_uncertainties
Denby B and Gola G (2010). Calculation of pseudo PM2.5 annual mean concentrations in Europe based on annual mean PM10 concentrations and other supplementary data. ETC/ACC Technical Paper 2010/9. http://air-climate.eionet.europa.eu/reports/ETCACC_TP_2010_9_pseudo_PM2.5_stations
De Smet P, Horálek J, Coňková M, Kurfürst P, de Leeuw F, Denby B (2009). European air quality maps of ozone and PM10 for 2006 and their uncertainty analysis. ETC/ACC Technical Paper 2008/8. http://air-climate.eionet.europa.eu/reports/ETCACC_TP_2008_8_spatAQmaps_2006
De Smet P, Horálek J, Coňková M, Kurfürst P, de Leeuw F, Denby B (2010). European air quality maps of ozone and PM10 for 2007 and their uncertainty analysis. ETC/ACC Technical Paper 2009/9. http://air-climate.eionet.europa.eu/reports/ETCACC_TP_2009_9_spatAQmaps_2007
EC (2008). Directive 2008/50/EC of the European Parliament and of the Council of 21 May 2008 on ambient air quality and cleaner air for Europe. OJ L 152, 11.06.2008, 1-44. http://eur-lex.europa.eu/LexUriServ/LexUriServ.do?uri=OJ:L:2008:152:0001:0044:EN:PDF
ECMWF: Meteorological Archival and Retrieval System (MARS). It is the main repository of meteorological data at ECMWF (European Centre for Medium-Range Weather Forecasts). http://www.ecmwf.int/
EEA (2010). Corine land cover 2000 (CLC2000) raster data. 100x100m gridded version 13 (2/2010); CLC 2000 V13 – 100m, g100_00.zip. http://www.eea.europa.eu/data-and-maps/data/corine-land-cover-2000-raster
EMEP (2008). Transboundary Particulate Matter in Europe: Status Report 2008. EMEP Status Report 4/2008. http://www.emep.int/publ/common_publications.html
ETC/LUSI (2010). Preliminary Corine Land cover 2000 (CLC2000) data for Switzerland. Personal communication.
Eurostat (2008). Total population for European states for 2008. http://epp.eurostat.ec.europa.eu/tgm/table.do?tab=table&language=en&pcode=tps00001&tableSelection=1&footnotes=yes&labeling=labels&plugin=1
Fagerli H, Simpson D, Tsyro S (2004). Unified EMEP model: Updates. In: EMEP Report 1/2004. MSC-W, Oslo, Norway. www.emep.int/publ/reports/2004/Status_report_int_del1.pdf

Horálek J, Kurfürst P, Denby B, de Smet P, de Leeuw F, Brabec M, Fiala J (2005). Interpolation and assimilation methods for European scale air quality assessment and mapping. Part II: Development and testing new methodologies. ETC/ACC Technical paper 2005/8. http://air-climate.eionet.europa.eu/docs/ETCACC_TechnPaper_2005_8_SpatAQ_Part_II.pdf

Horálek J, Denby B, de Smet PAM, de Leeuw FAAM, Kurfürst P, Swart R, van Noije T (2007). Spatial mapping of air quality for European scale assessment. ETC/ACC Technical paper 2006/6. http://air-climate.eionet.europa.eu/docs/ETCACC_TechnPaper_2006_6_Spat_AQ.pdf

Horálek J, de Smet PAM, de Leeuw FAAM, Denby B, Kurfürst P, Swart R, (2008). European air quality maps including uncertainty analysis. ETC/ACC Technical paper 2007/7. http://air-climate.eionet.europa.eu/reports/ETCACC_TP_2007_7_spatAQmaps_ann_interpol

Horálek J, de Smet PAM, de Leeuw FAAM, Coňková M, Denby B, Kurfürst P (2010). Methodological improvements on interpolating European air quality maps. ETC/ACC Technical Paper 2009/16. http://air-climate.eionet.europa.eu/reports/ETCACC_TP_2009_16_Improv_SpatAQmapping

Jimmink B, de Leeuw F, Noordijk E, Ostatnická J, Coňková M (2010). Reportingon ambient air quality assessment in the EU Member States, 2008. ETC/ACC Technical Paper 2010/11. http://air-climate.eionet.europa.eu/reports/ETCACC_TP2010_11_AQQ2008

JRC population density data (2009). Population density disaggregated with Corine land cover 2000. 100x100 m grid resolution, EEA version pop01clcv5.tif of 24 Sep 2009. http://www.eea.europa.eu/data-and-maps/data/population-density-disaggregated-with-corine-land-cover-2000-2

Mareckova K, Wankmueller R, Pazdernik K, Purzner M, Zechmeister A, Joebstl R, Adams M (2010). Inventory Review 2010. Review of emission data reported under the LRTAP Convention and NEC Directive. Stage 1 and 2 Review. Technical Report CEIP 1/2010. http://www.ceip.at/fileadmin/inhalte/emep/pdf/2010/Inventory_Review_2010.pdf

Mol WJA, van Hooydonk PR, de Leeuw FAAM (2010). European exchange of monitoring information and state of the air quality in 2008. ETC/ACC Technical Paper 2010/1. http://air-climate.eionet.europa.eu/reports/ETCACC_TP_2010_1_EoI_AQ_meta_info2008

ORNL (2002). ORNL LandScan 2002 Global Population dataset. http://www.ornl.gov/sci/landscan/landscanCommon/landscan02_release.html

Simpson D, Fagerli H, Jonson JE, Tsyro S, Wind P, Tuovinen J-P (2003). Transboundary acidification and eutrophication and ground level ozone in Europe: Unified EMEP model description. EMEP Status Report 1/03 Part I. MNP, Oslo, Norway. http://www.emep.int/publ/reports/2003/emep_report_1_part1_2003.pdf

Tarrasón L, Nyíri Á. (2008). Transboundary acidification, eutrophication and ground level ozone in Europe in 2006. EMEP Status Report 1/2008. http://www.emep.int/publ/common_publications.html

UNECE (2004). Mapping Manual 2004. Manual on methodologies and criteria for Modelling and Mapping Critical Loads and Levels and Air Pollution Effects, Risks and Trends. United Nations – Economic Commission for Europe, LRTAP Convention. http://www.oekodata.com/icpmapping/htm/manual/manual_eng.htm

UN (2007). World Population Prospects - The 2006 Revision, Highlights. United Nations. Department of Economic and Social Affairs, Population Division. New York. http://www.un.org/esa/population/publications/wpp2006/WPP2006_Highlights_rev.pdf

Vixseboxse E, De Leeuw F (2009). 2007 Annual Member States reporting on ambient air quality assessment – 'The Questionnaire'. ETC/ACC Technical Paper 2009/2. http://air-climate.eionet.europa.eu/reports/ETCACC_TP2009_2_AQQ2007